Article

Sensitivity of Different Parameterizations on Simulation of Tropical Cyclone Durian over the South China Sea using Weather Research and Forecasting (WRF) model

Worachat Wannawong [1,*], Donghai Wang [1], Yu Zhang [1] and Chaiwat Ekkawatpanit [2]

[1] School of Atmospheric Sciences, Sun Yat-sen University, Guangzhou 510275, China
[2] Department of Civil Engineering, Faculty of Engineering, King Mongkut's University of Technology Thonburi, Bangkok 10140, Thailand
* Correspondence: worachataj@hotmail.com; Tel.: +86-131-4311-3438

Abstract: Typhoon Durian forming over the Western North Pacific Ocean and entering into the South China Sea (SCS), caused extreme and widespread damages in 2006. In this research, sensitivity analyses on different physical parameterization schemes of the Weather Research and Forecasting Atmospheric Model (WRF-ATM) have been utilized to study typhoon Durian. Model accuracy and performance testing were investigated with different initial conditions during the tropical cyclone simulation in the SCS. The initial and boundary conditions (IBCs) for all experiments were derived from the European Centre for Medium Range Weather Forecasts (ECMWF), Re-Analysis Interim (ERAI), and the National Centers for Environmental Prediction (NCEP) with Final (FNL) analysis data compiled through the WRF-ATM model. The sensitivity analysis results indicated a major improvement for the cumulus scheme by using the Grell-Devenyi scheme along with the PBL scheme of Yonsei University, mixed-phase microphysics scheme of the WRF Single Moment 5-class and IBCs for ECMWF-ERAI of TC simulation under the context of Wind-Pressure Relationships. This predicted better track and intensity comparing with these of the Joint Typhoon Warning Center. The results revealed that the TC track and intensity were well simulated by the WSM5-GD combination for the WRF-ATM model with an intensity error of 1.69 hPa for minimum surface level pressure, maximum wind speed of 1.83 knots and average track error of 25 km in 72 hours. The simulations showed that the potential track and intensity error decreased with the delayed IBCs, suggesting that the model simulation is more dependable when the coast is approached by the TC.

Keywords: Typhoon Durian; Tropical cyclone; Wind-Pressure Relationships; South China Sea; Sensitivity analysis; WRF

1. Introduction

Severe Tropical Cyclones (TC) in the Western North Pacific (WNP) Ocean and the South China Sea (SCS) are one of the most destructive weather phenomena. Heavy rainfall, flooding, landslides, strong winds, low pressure, high waves, and storm surge are the major hazards associated with TC activities [1–3]. Loss of life and livelihoods caused by intense cyclones could be substantially reduced by appropriate mitigation strategies including accurate and long lead forecasting. Recently, the model studies as well as the Weather Research and Forecasting Atmospheric Model (WRF-ATM) have been used to examine the TC mechanism induced by the atmospheric and oceanic conditions,

e.g., the Sea Surface Temperature (SST) and heat fluxed changes at the surface over the WNP Ocean and the SCS [4]. The WRF-ATM model is the regional Numerical Weather Prediction (NWP) model which can be used to predict the meteorological phenomena - including the TC potential track and its intensity. It is one of the most well-known numerical weather prediction models in mesoscale simulation systems. In addition, the WRF-ATM model is not only able to be used for simulation of real and ideal cases, but also in providing various physical parameterizations for a theoretical basis to study the physical process and integration with multiple models as in a fully coupled model [5]. This model uses initial boundary conditions (IBCs) to solve the dynamical atmospheric and thermodynamic equations with the assumptions of some physics options. The model simulations for the scale analysis as in the mesoscale predictions are highly sensitive to the physical parameterizations used in model forecasting with complex topography, especially in the SCS. Cumulus convection and boundary layer physics play an important role in the development and intensification of TC prediction. Although parameterization schemes have some limitations on the prediction of the TC track and its intensity, they play a very crucial role in weather event simulations.

The sensitivity study is, therefore, an approach to identify the impact of different physical parameterizations and IBCs on the TC track and intensity simulation under the Wind–Pressure Relationships (WPRs) with a smooth curve for the statistical validation of model simulations and observation. In recent years, Islam et al. [6] studied the sensitivity of model physical parameterizations on simulation of super typhoon Haiyan 2013 over the WNP Ocean by using two different datasets from the European Centre for Medium Range Weather Forecasts (ECMWF), Re-Analysis Interim (ERAI) and the National Centers for Environmental Prediction (NCEP) Global Forecast System (GFS) data. Their study suggested that the best choice of physical combination and parameterization for the typhoon Haiyan case study is in the WNP Ocean under the WPRs for the comparison of model simulations and observation. The simulation results were compared with the best track obtained from the Joint Typhoon Warning Centre (JTWC) based on the criteria of Root Mean Square Error (RMSE). It was found that the lowest intensity error was 4.21 hPa for Minimum Surface Level Pressure (MSLP), Maximum wind speed (V_{max}) was 3.26 knots and average track error was 87.33 km in 48 hours forecasted by using the WRF single moment 6-class (WSM6) for microphysics scheme with the Quasi-Normal Scale Elimination (QNSE) for the Planetary Boundary Layer (PBL) combination. Other sensitivity studies related to the WRF-ATM physical parameterizations can be found in Srivastava et al. [7] and Mooney et al. [8].

For the study cases with the performance testing, Wang [9] presented that a high-resolution model results showed its performance for TC simulations. A high-resolution experiment using nested grids of 15-km and 5-km grid spacing with 183×195 and 267×273 grid points, respectively, had been set up in order to better investigate the impact of the vortex relocation on the intensity forecast. A better definition of the initial vortex was found as a major reason for the TC track and its intensity improvements for a short-term prediction. For long-term simulations, the WRF-ATM model with TC simulation results was also widely used in the WNP Ocean [4].

In this research, super typhoon Durian (2006) has been used as a case study. Its track spanned 15 days without a decrease of TC's primary energy after passing the Philippines. It continued heading toward the SCS to the Gulf of Thailand (GoT) and the onwards to the Bay of Bengal (BoB). It was also classified as one of two typhoons showing strong power crossing the North-West Pacific Ocean into the BoB. In this work, TC activities including wind and pressure changes have been investigated by using the SST update under the surrounding oceanic environments, different physical parameterizations, and IBCs. The impact on TC position tracking and intensity were also studied. In addition, to our knowledge, the sensitivity analysis of different parameterizations on super typhoon Durian using WRF-ATM model has not been studied. The present work, therefore, aimed at investigating for the sensitivity of physical parameterization schemes of super typhoon Durian over the SCS. The model accuracy and performance testing were also presented by using the WPRs of the WRF-ATM model simulations and best-track datasets.

Preprints (www.preprints.org) | NOT PEER-REVIEWED | Posted: 26 April 2018 doi:10.20944/preprints201804.0336.v1

2. Description of Typhoon, Model Configuration and Analysis

2.1. A Brief Overview of Super Typhoon Durian

Super typhoon Durian (category 4) was formed as a tropical depression at 1200 UTC 24 November 2006 which was reported by the JTWC. The pre-Durian disturbance was tracked at the initial location of 6.1° N, 149.8° E. The tropical depression intensity slowly intensified and moved west to west-northwestward with V_{max} of 15 knots and MSLP of 1006 hPa. Its intensity was upgraded from tropical depression to tropical storm at 0600 UTC on 26 November with V_{max} of 35 knots and MSLP of 997 hPa at the location of 9.7° N, 142.8° E. A few days later, it developed rapidly, achieving typhoon strength and acquiring the name Durian at 1200 UTC on 28 November with V_{max} of 65 knots and MSLP of 976 hPa at the location of 12.1° N, 131.6° E according to the JTWC records. Its intensity was then upgraded to a category 4 Super Typhoon at 1200 UTC on 29 November and 0000 UTC on 30 November. In this study, the model experiments and their simulations were used to validate with the JTWC best-track data. The model simulations were conducted between 0000 UTC 2 December to 0000 UTC 5 December 2006 covering a period of Durian intensity in the SCS as shown in Figure 1.

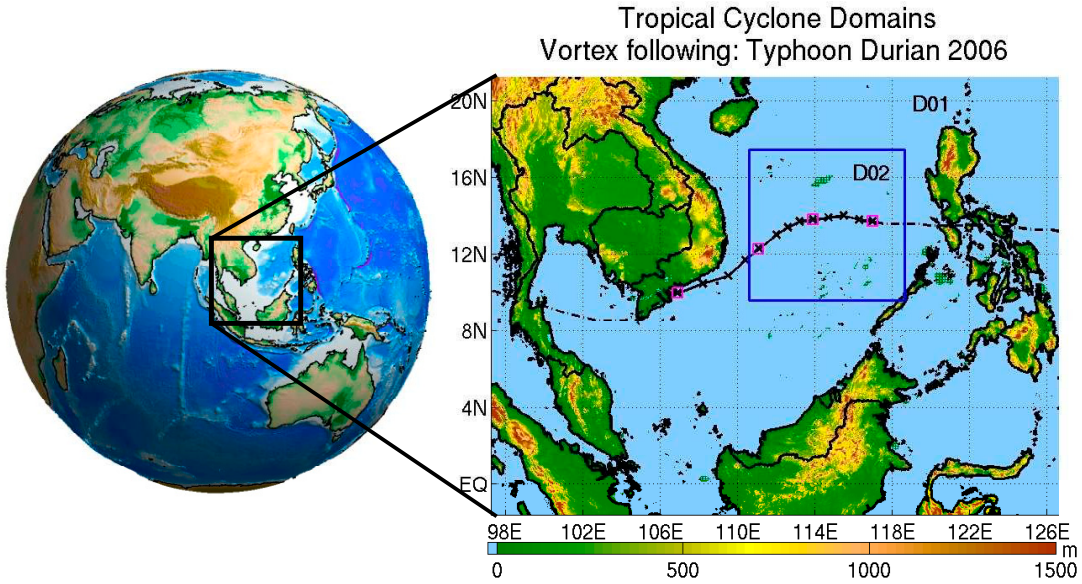

Figure 1. Study domains (D01 and D02) of WRF-ATM model, associated with JTWC best track data from 0000 UTC 2 December to 0000 UTC 5 December 2006. The daily intervals of track locations are shown in the pink squares.

2.2. Model Description and Configuration

The WRF-ATM model version 3.7.1 [10] was applied in this study. This model version is part of a full package of coupled modeling systems [5]. In this work, the WRF-ATM model was built with the Automated Tropical Cyclone Forecasting (ATCF) two-way vortex-following the moving nested grid domains for a short-term simulation. The study domain was configured at the center point of 10° N, 112° E (latitude-longitude). A two-way nesting was employed or the interaction between outer and inner domains as shown in Figure 1. The parent domain has been set up for 219×174 grid points with a 15-km grid spacing, while the child domain has been set up for 180×180 grid points with a 5-km grid spacing as shown in Table 1. The NCEP-Final (FNL) reanalysis and ECMWF-ERAI global model datasets were used to provide the IBCs with 30 terrain following and the top of model at 50 hPa for both domains in the WRF-ATM experimental simulations. The model studies have been illustrated by the different IBCs global model datasets with physics options combination. The model results with sensitivity analysis by physical parameterizations and performance testing have been compared with the JTWC best-track data under the WPRs (Table 2).

Preprints (www.preprints.org) | NOT PEER-REVIEWED | Posted: 26 April 2018 doi:10.20944/preprints201804.0336.v1

127 **Table 1.** Model configuration of WRF-ATM

Model setup	Information
Grid points	Outer domain: 221x174 (D01)
	Inner domain: 180x180 (D02)
Horizontal resolution	Outer domain: 15 km (D01)
	Inner domain : 5 km (D02)
Vertical resolution	30 layers;
	Model top set to 50 hPa
Centered domain	11°N, 113°E
Time step	90 sec
Map projection	Mercator
IC/BCs	1. ECMWF-ERAI:
	1.1 6-h time interval by ERAI
	1.2 Daily ERAI-SST averaged from ECMWF
	1.3 0.75°×0.75° horizontal and 61 vertical grid resolutions
	2. NCEP-FNL:
	2.1 6-h time interval by FNL
	2.2 Daily RTG-SST updated from NCEP/NOAA
	2.3 1.0°×1.0° horizontal and 27 vertical grid resolutions
Simulation/Spin-up periods	3. ECMWF-ERAI:
	3.1 0000 UTC 01 Dec–0000 UTC 06 Dec/1 day
	3.2 1200 UTC 01 Dec–0000 UTC 06 Dec/0.5 days
	4. NCEP-FNL:
	4.1 0000 UTC 01 Dec–0000 UTC 06 Dec/1 day
	4.2 1200 UTC 30 Nov–0000 UTC 06 Dec/1.5 days

128

129 **Table 2.** Differences of physical parameterizations of WRF-ATM model sensitivity analysis

Experiment	Microphysics	Cumulus	PBL	LW radiation	SW radiation	Surface layer	Land surface
Exp.I	WSM5	KF	YSU	RRTM	Dudhia	MM5	Noah
Exp.II	WSM5	BMJ	YSU	RRTM	Dudhia	MM5	Noah
Exp.III	WSM5	GD	YSU	RRTM	Dudhia	MM5	Noah
Exp.IV	WSM6	KF	YSU	RRTM	Dudhia	MM5	Noah
Exp.V	WSM6	BMJ	YSU	RRTM	Dudhia	MM5	Noah
Exp.VI	WSM6	GD	YSU	RRTM	Dudhia	MM5	Noah
Exp.VII	THOM	KF	YSU	RRTM	Dudhia	MM5	Noah
Exp.VIII	THOM	BMJ	YSU	RRTM	Dudhia	MM5	Noah
Exp.IX	THOM	GD	YSU	RRTM	Dudhia	MM5	Noah

130

131

 doi:10.20944/preprints201804.0336.v1

2.3. Initial and Lateral Boundary Conditions

For the IBCs, the WRF-ATM model is used to downscale from the ECMWF-ERAI global scale-reanalysis data with 0.75°×0.75° horizontal and 61 vertical grids to the regional grid domains of all model experiments at 15 and 5 km resolutions. The main feature of the ECMWF-ERAI global model has been improved by the 4DVAR data assimilation, while the 3DVAR data assimilation has been using for the NCEP-FNL model components and analysis. The ECMWF-ERAI time range covers from 1979 to present and the SST has also been included, whereas the NCEP-FNL models time range covers from 1999 to present. The resolution of ECMWF-ERAI meteorological grid level in horizontal and vertical coordinates are finer than the NCEP-FNL reanalysis data with 1.0°×1.0° horizontal and 27 vertical grids. The model recommendation for the WRF-ATM model modification with the NCEP-FNL model data has been updated by the Real-Time Global (RTG)-SST with the 0.5°×0.5° horizontal grids.

In this study, the model configuration has been applied for two-way vortex-following moving nested grids and modeled feedback between both domains with the TC model experiments and numerical simulations. The two-way nesting was available for the model interaction between both domains with the ATCF.

Figure 1 illustrates the D01-outer and D02-inner domains with parent and child domains, which covered some parts of the Indochinese Peninsula (IP) including the SCS and GoT. For all model experiments, both ECMWF-ERAI and NCEP-FNL datasets were available as 6-hour reanalysis data, which has been used for the WRF-ATM IBCs model. Figures 2–4 show the sample initial datasets and differences of ECMWF-ERAI and NCEP-FNL for wind, sea level pressure and SST fields from 0000 UTC 2 December to 0000 UTC 4 December 2006. This data has been used as the initial data for the model integration of nine experimental designs with different IBCs and model spin-up periods for 36 case studies. It was performed without observation assimilation as shown in Tables 1 and 2. The model consideration began at 0000 UTC 2 December 2006, and continued until 0000 UTC 5 December 2006 with different spin-up times. The first experiment with 24 hour (1 day) forecast was considered for the model spin-up time. The second experiment for different spin-up running with 12 hours (0.5 days) and 36 hours (1.5 days) forecasts were also mainly discussed by the average daily weather considerations. Another model experiment of the WRF model with the differences of ERAI and FNL IBCs for 1.5 and 0.5 day spin-up periods were not presented here.

Preprints (www.preprints.org) | NOT PEER-REVIEWED | Posted: 26 April 2018 doi:10.20944/preprints201804.0336.v1

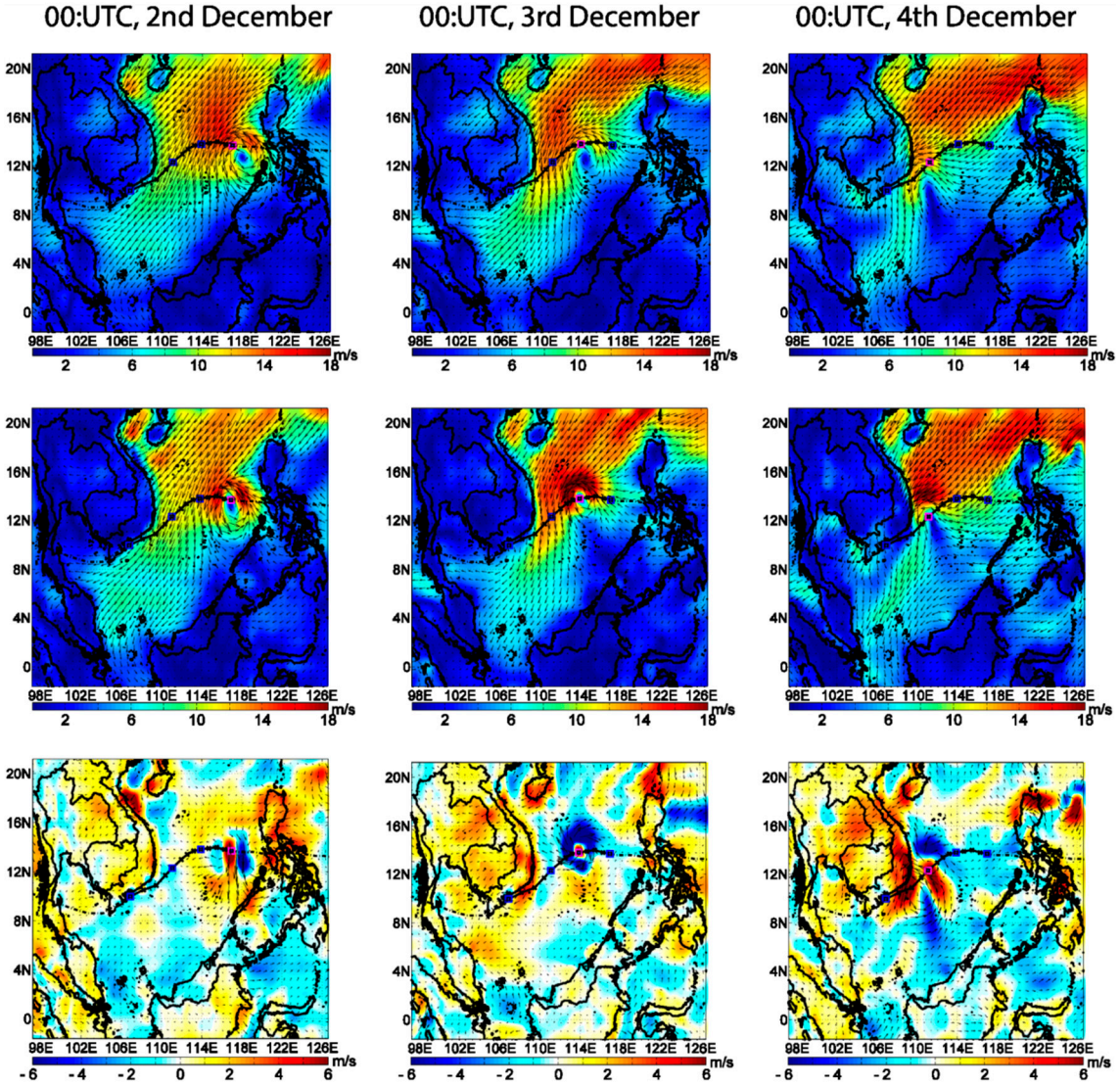

Figure 2. Sample IBCs of wind fields (m/s) at the 10-meter height level. ECMWF-ERAI (top row), NCEP-FNL (middle row), and difference of both IBCs (bottom row) from 0000 UTC 2 December to 0000 UTC 4 December 2006.

Preprints (www.preprints.org) | NOT PEER-REVIEWED | Posted: 26 April 2018 doi:10.20944/preprints201804.0336.v1

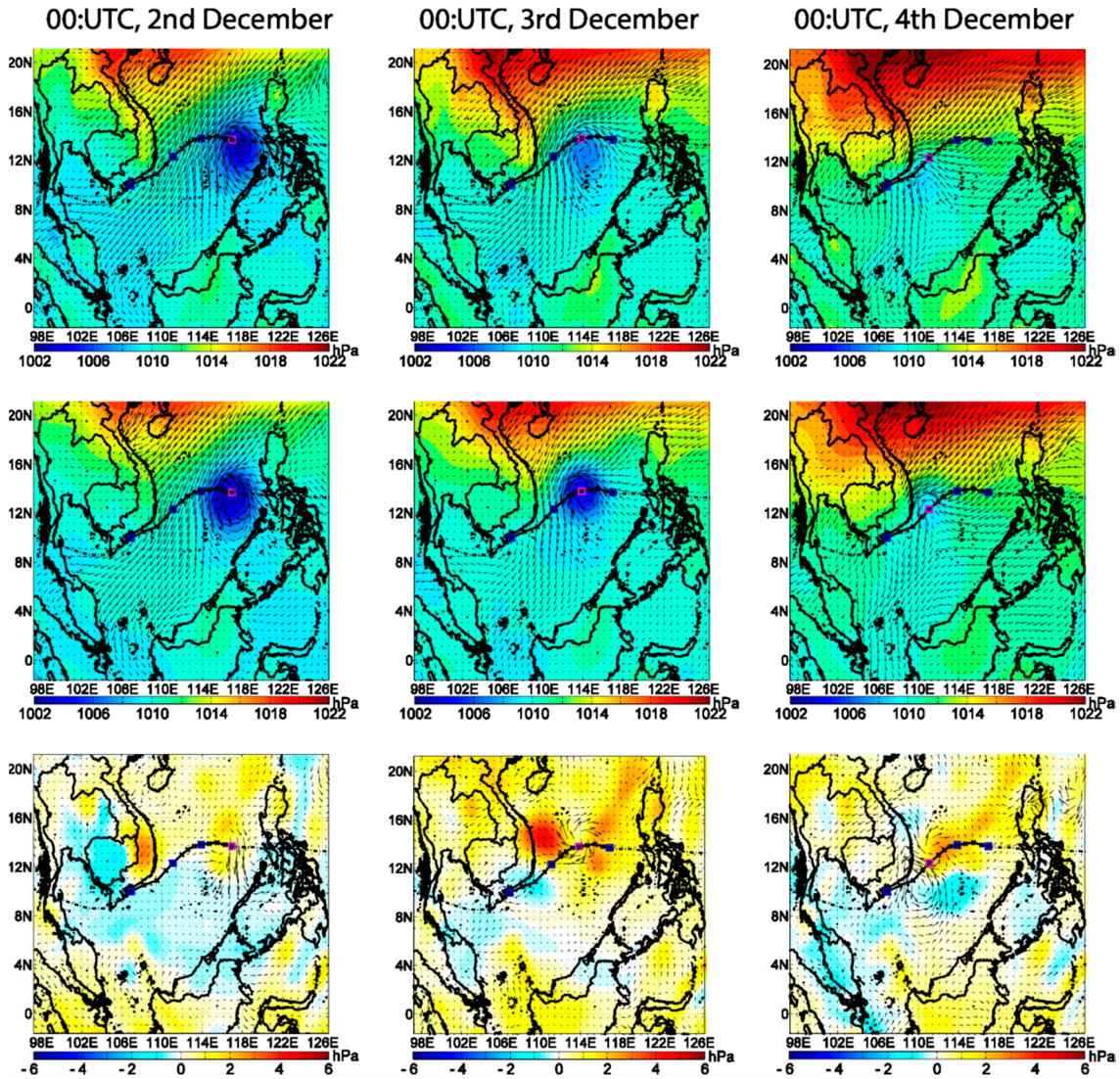

167 **Figure 3.** As in Figure 2, but for surface level pressure (hPa).

168

Preprints (www.preprints.org) | NOT PEER-REVIEWED | Posted: 26 April 2018 doi:10.20944/preprints201804.0336.v1

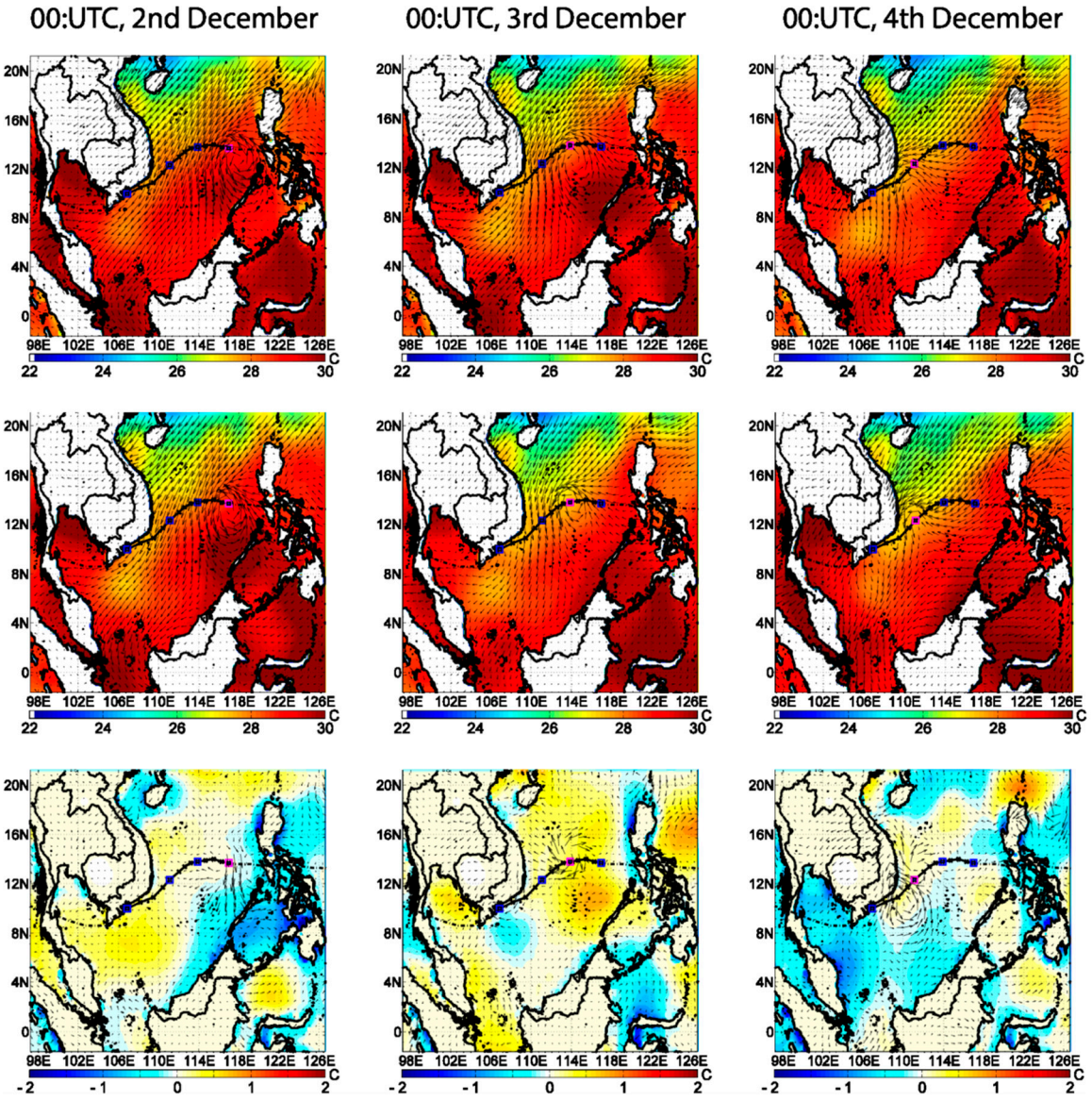

Figure 4. As in Figure 3, but for sea surface temperature (°C).

2.4. Physical Parameterizations of Model Simulation

The impact of model physics options on TC simulations was described in this study. These physical parameterizations and their combinations were conducted for two major physics schemes - Microphysics (MP) and Cumulus (Cu) parameterizations with specific Planetary Boundary Layer (PBL) for nine experiments (Experiment I to Experiment IX). The best choice of physics options was investigated by using both IBCs for the model accuracy and performance testing as summarized in Table 2.

For the first sensitivity analysis, the WRF-ATM experimental models were designed for three different combinations to study the differences of MP and Cu schemes by the TC simulations. The MP schemes provided the atmospheric heat and moisture tendencies with the vertical flux of cloud, precipitation and sedimentation processes of hydrometeors [11]. The MP scheme determinations widely used in the WRF-ATM model community included the WRF Single Moment 5-class (WSM5), WRF Single Moment 6-class (WSM6), and Thompson (THOM) schemes [10]. The WSM5 scheme was updated from the original scheme, viz., the WRF Single Moment 3-class (WSM3). It was also allowed for the mixed-phase processes of cloud water/ice, rain, snow and super-cooled water. The WSM5 scheme was chosen after some initial tests showing that this scheme agreed well with the more complicated MP schemes.

Preprints (www.preprints.org) | NOT PEER-REVIEWED | Posted: 26 April 2018 doi:10.20944/preprints201804.0336.v1

For the newly issued conceptual framework of WSM, graupel was introduced as another variable which measured a new combined snow/graupel fall speed in the WSM6 scheme, while the ice number concentration still followed the concept of WSM3 and WSM5 schemes [12]. In addition, the new THOM scheme [13] was applied to study the impacts of MP schemes in the final application of this section. The generalized gamma distribution shape of each hydrometeor species by the new THOM scheme distributed the new snow parameterization depending upon both ice/water content and temperature. A summary of overall analysis, the MP schemes have been accompanied by the Yonsei University (YSU) PBL scheme [14]. The MM5 surface layer, Noah Land Surface Model (LSM), Long-Rapid Radiative Transfer Model (RRTM) and short wave radiation schemes were also required [15] as described in Table 2.

It was found that the Cu schemes were not kept fixed (Table 2). The model experimental simulations were applied for three Cu-schemes. The first Cu-scheme was started by the Kain-Fritsch (KF) [16]. For deep tropical convection, the Betts-Miller-Janjic (BMJ) scheme provides the characteristic profiles of temperature and moisture. The deep convection profiles are proportional to the entropy change, precipitation, mean cloud temperature and efficiency, while the shallow convection moisture profile requires a non-negative change of entropy [17]. For the last Cu scheme, the Grell-Devenyi (GD) scheme [18] has been simplified for the modified quasi-equilibrium assumption and equilibrium in the mass flux scheme. The GD scheme is based on the Convective Available Potential Energy (CAPE), low-level vertical velocity and moisture convergence, thickness of the capping inversion and the dependence of the downdraft on the precipitation efficiency, leading to more variability in the ensemble spread. The ensemble spread is introduced by effective multiple Cu schemes and variants which run within each grid box. It is also averaged to provide feedback to the model.

However, the TC sensitivity analysis only examined YSU for the PBL physical parameterizations and also kept fixed for the Rapid Radiative Transfer Model (RRTM) Long Wave (LW) radiation [19], Dudhia shortwave radiation schemes [20], MM5 similarity surface layer, and the Noah Land Surface Model [15].

2.5. Statistical Verification and Operational Agency Equations

In this research, the TC experiments were simulated in nine physical combinations with two different IBCs and spin-up periods by the ATCF two-way vortex-following moving nested grid domains for the sensitivity study and analysis as shown in Tables 1 and 2 for 36 case studies. These studies were classified by the intensity of V_{max}, MSLP and potential track area under the WPRs through the WRF-ATM model experiments. In this section, the main state was to validate the model simulations with the JTWC best-track data. The TC model experiments were also reanalyzed by exhibiting a smooth descending trend of V_{max} and MSLP with the operational agency equations to represent the real state of the simulation variables. Three statistical indexes, which were Bias, Root Mean Squared Error (RMSE), and Standard Deviation Error (STDE), with five operational agency equations (Opa.I–Opa.V) were utilized for model accuracy evaluation and performance testing. Equations used by the operational center agencies are as follows.

The equation for the National Hurricane Center/Tropical Prediction Center and the Central Pacific Hurricane Center/Operational agency (Opa.I) has been applied from the Dvorak [21] equation:

$$\mathrm{MSLP} = 1{,}021.36 - 0.36\mathrm{V}_{max} - \left(\mathrm{V}_{max} / 20.16\right)^2 \quad (1)$$

The equation used by the Regional Specialized Meteorological Center (RSMC)/Operational agency (Opa.II) in Tokyo has been adapted from the Knaff and Zehr [22] equation or Koba equation:

$$\mathrm{MSLP} = 6.22 - 0.58\mathrm{V}_{max} - \left(\mathrm{V}_{max} / 31.62\right)^2 + 1{,}010 \quad (2)$$

Preprints (www.preprints.org) | NOT PEER-REVIEWED | Posted: 26 April 2018 doi:10.20944/preprints201804.0336.v1

The RSMC La Reunion Island, RSMC Fiji, Perth Tropical Cyclone Center, and Joint Typhoon Warning Center (JTWC)/Operational agency (Opa.III) have followed the Atkinson and Holliday [23] equation:

$$\mathrm{MSLP} = -\left(\mathrm{V}_{max} / 6.7\right)^{1.553} + 1{,}010 \quad (3)$$

The Darwin Center/Operational agency (Opa.IV) applied the Love and Murphy [22] equation:

$$\mathrm{MSLP} = 6.37 - 0.54\mathrm{V}_{max} - \left(\mathrm{V}_{max} / 43.03\right)^{2} + 1{,}010 \quad (4)$$

The equation used by the Brisbane Center/Operational agency (Opa.V) is applied from the Crane [22] equation:

$$\mathrm{MSLP} = 5.82 - 0.50\mathrm{V}_{max} - \left(\mathrm{V}_{max} / 22.20\right)^{2} + 1{,}010 \quad (5)$$

where V_{max} is the maximum surface wind (in knots) and MSLP is the minimum surface level pressure (in hPa).

3. Interpretation of Model Simulation Results

The TC potential track and its intensity have been considered to be the most important and challenging contents for the NWP systems. The model accuracy of TC tracking is most crucial to examine the geographical location where actual damages due to TC intensity such as strong wind associated with low pressure. Misinformation from the TC center by the NWP system would produce inaccurate TC tracking and its intensity with circulation at the actual location on land and sea. Therefore, the TC simulation testing through WRF–ATM model experiments and its sensitivity analysis are essential to locate areas of TC intensities in the SCS. In section 3.1, the impact of different physical parameterization schemes for the TC predictions is discussed.

3.1. Impact of Microphysics and Cumulus Combination Schemes

The TC track and its intensity prediction of three KF, BMJ, and GD Cu-convective schemes with combination of three WSM5, WSM6 and THOM MP-schemes are discussed in this section. Figures 5 and 6 show nine-experimental designs of TC Durian simulations of location tracking (top panel) and its intensity as V_{max} (middle panel) and MSLP (bottom panel) associated with the JTWC observed track, different IBCs and spin-up periods.

Preprints (www.preprints.org) | NOT PEER-REVIEWED | Posted: 26 April 2018 doi:10.20944/preprints201804.0336.v1

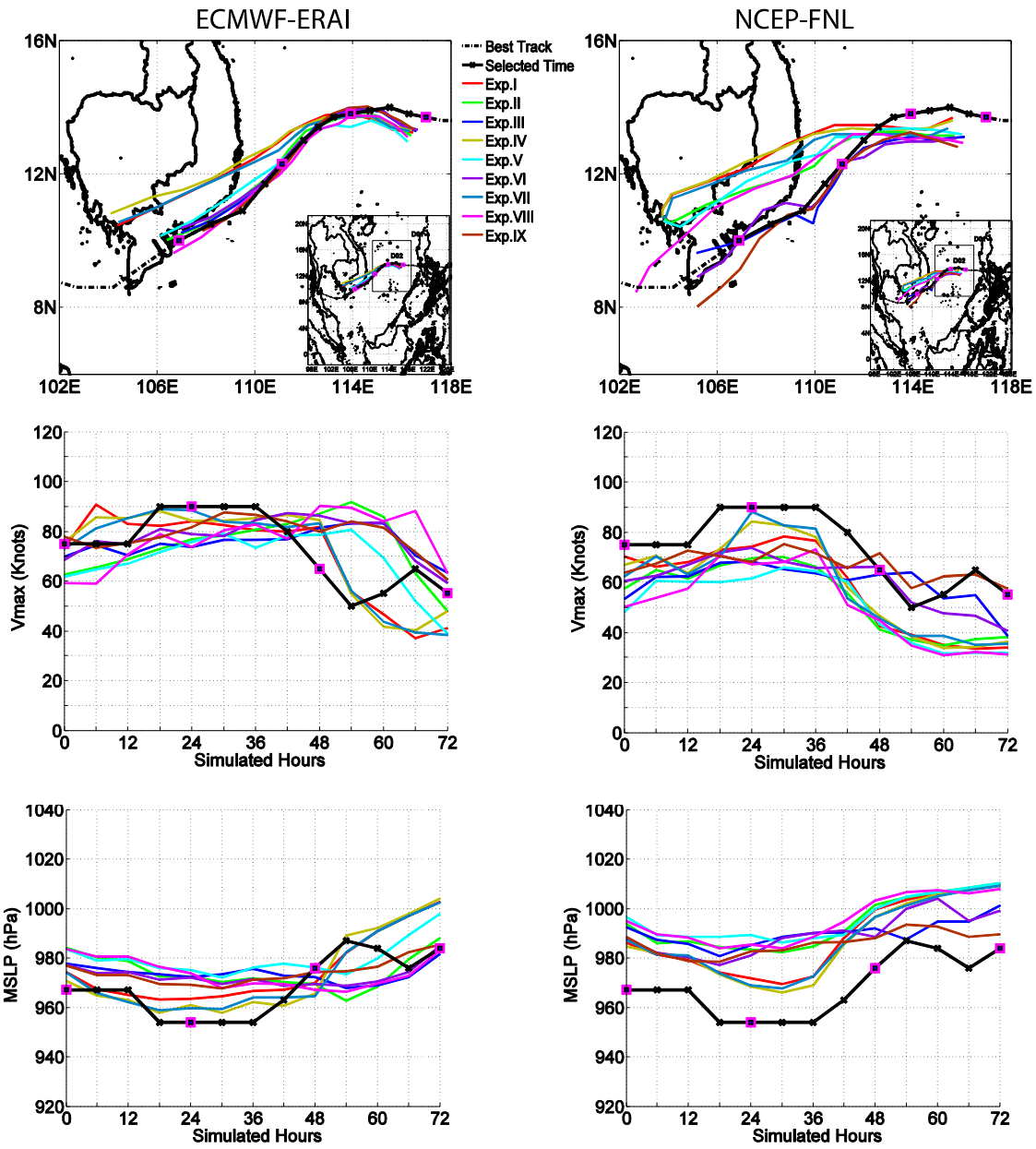

Figure 5. Time series of ECMWF-ERAI (left column) and NCEP-FNL IBCs (right column) by using WRF-ATM model simulations, associated with JTWC best-track data. TC potential track simulations (top row), V_{max} (knots) (middle row), and MSLP (hPa) (bottom row). The daily intervals of track locations are shown in the pink squares from 0000 UTC 2 December to 0000 UTC 5 December 2006 (1 day spin-up time).

Preprints (www.preprints.org) | NOT PEER-REVIEWED | Posted: 26 April 2018 doi:10.20944/preprints201804.0336.v1

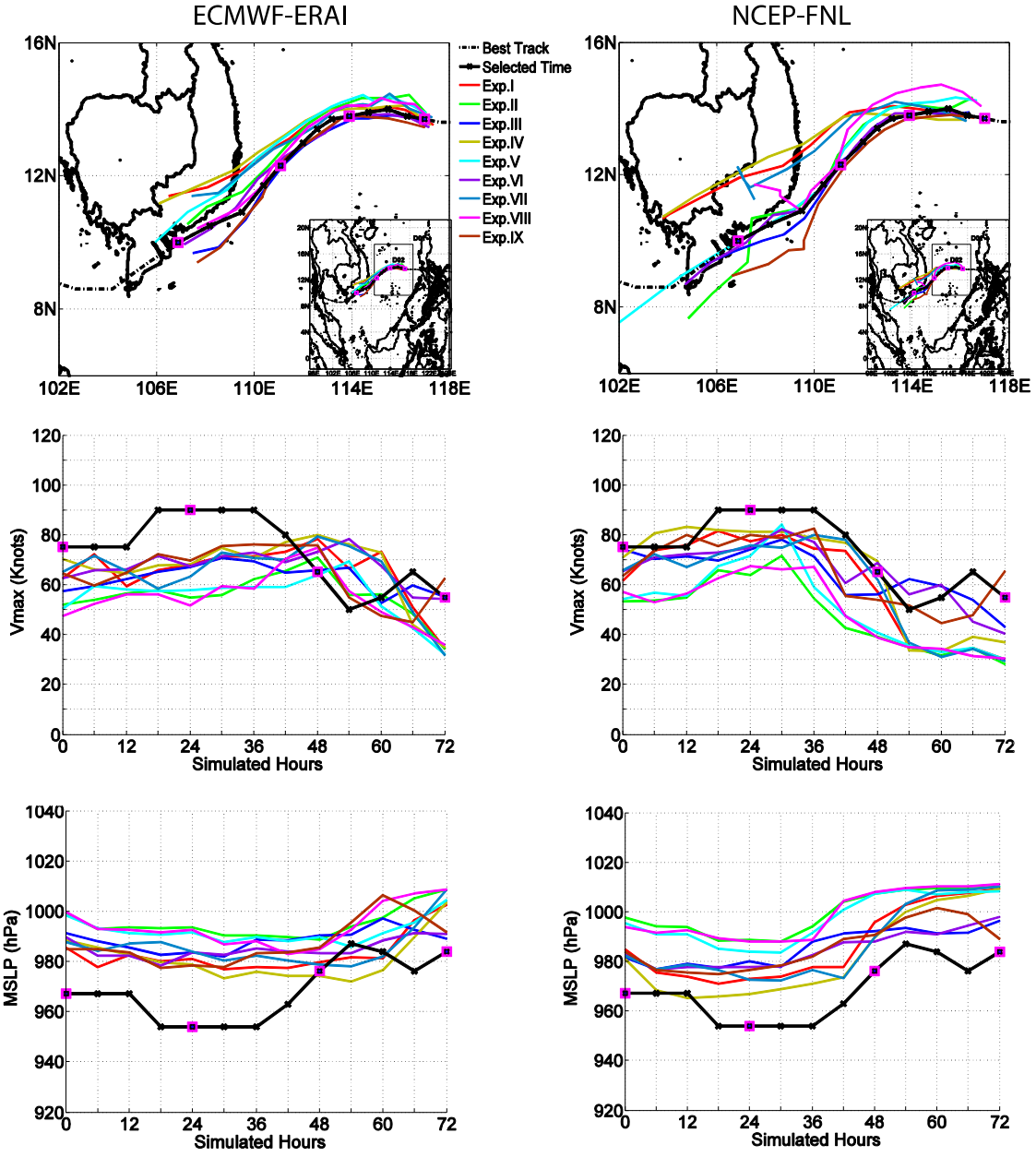

Figure 6. As in Figure 5, but for different model spin-up times, 0.5 days for ECMWF-ERAI (left panel) and 1.5 days for NCEP-FNL IBCs (right panel).

The GD combinations showed better TC location tracking with a group of three MP schemes comparing with the JTWC best-track data, especially for a physical combination of WSM5 MP-scheme (Experiment III) by using the ECMWF-ERAI IBCs of one day spin-up period on a specific model driving. However, the GD scheme with a combination of three MP schemes fails at the strong influence of upwelling area with high SST variability [24,25] as in the South-eastern Coast of Vietnam (SCOV). The vector displacement error for TC simulated tracks with above stated schemes are demonstrated in Tables 3 and 4, as well as those two figures in the top panel of Figures 5 and 6.

Preprints (www.preprints.org) | NOT PEER-REVIEWED | Posted: 26 April 2018 doi:10.20944/preprints201804.0336.v1

279 **Table 3.** Daily average track errors (in km) of model experiments derived by ECMWF-ERAI IBCs with different
280 simulation/spin-up periods, associated with JTWC best-track achieves.

Experiment	1 day spin-up period				0.5 days spin-up period			
	Day 1	Day 2	Day 3	Avg.	Day 1	Day 2	Day 3	Avg.
Exp.I	93	117	229	146.3	27	71	127	75.1
Exp.II	76	66	66	69.3	54	82	72	69.1
Exp.III	39	15	22	25.3	21	24	46	30.1
Exp.IV	100	138	255	164.3	26	68	133	75.5
Exp.V	97	69	68	78.0	49	84	100	77.9
Exp.VI	37	16	28	27.0	21	30	29	26.7
Exp.VII	94	115	231	146.7	42	91	136	90.0
Exp.VIII	78	60	55	64.3	55	82	101	79.2
Exp.IX	40	20	59	39.7	26	40	79	48.3

281

282 **Table 4.** As in Table 3, but derived by NCEP-FNL IC/BCs.

Experiment	1 day spin-up period				1.5 days spin-up period			
	Day 1	Day 2	Day 3	Avg.	Day 1	Day 2	Day 3	Avg.
Exp.I	219	319	478	338.7	131	215	381	242.5
Exp.II	216	339	480	345.0	77	185	320	194.3
Exp.III	198	269	186	217.7	113	210	216	179.5
Exp.IV	224	334	484	347.3	156	250	417	274.3
Exp.V	202	314	468	328.0	81	174	404	219.9
Exp.VI	210	261	209	226.7	124	210	271	201.6
Exp.VII	230	329	475	344.7	129	202	254	194.9
Exp.VIII	209	324	503	345.3	79	127	146	117.1
Exp.IX	203	287	320	270.0	90	207	187	161.5

Preprints (www.preprints.org) | NOT PEER-REVIEWED | Posted: 26 April 2018 doi:10.20944/preprints201804.0336.v1

A summary of TC tracking error under the differences of IBCs and spin-up period conditions is shown in Figure 7. The GD scheme showed a small tracking error increasing after 48 hours of simulation testing comparing with the JTWC best track data and other Cu-schemes. Therefore, the KF and BMJ schemes were eliminated in the selection of Cu-physical parameterization schemes for TC Durian simulation in the SCS. The KF and BMJ schemes created quite large tracking errors during the time of strong influence in the upwelling area with high SST variability by updating SST during the WRF-ATM model simulations in the SCOV (i.e. between 4 and 5 December 2006). The TC intensity was discussed in terms of MSLP and V_{max} with above stated set of combinations. General consideration and comparative study for model simulation (up to 72 hour forecast) and its approximation were presented in the middle and bottom panels of Figures 5 and 6 (i.e. V_{max} and lowest center of MSLP). The MSLP at the lowest center of JTWC observed data was around 976 hPa at 1800 UTC 4 December 2006 in the SCOV. It clearly showed that the GD combinations (Experiments III, VI and IX) were close to the observed central pressure (972.3, 974.4, and 982.4 hPa), especially one day spin-up time for the TC simulation by using the ECMWF-ERAI IBCs.

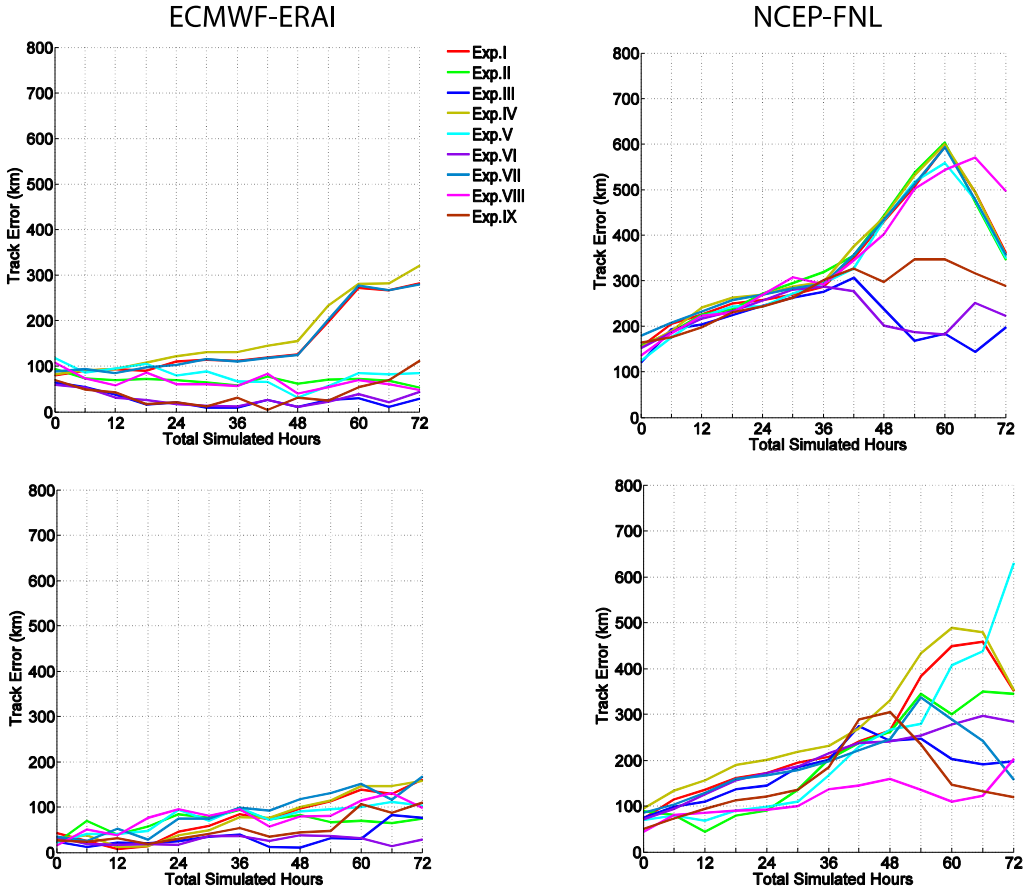

Figure 7. Track error (km) of model experiments and a comparison of ECMWF-ERAI (left column) and NCEP-FNL IBCs (right column); same (top row) and different (bottom row) spin-up periods by using the WRF-ATM model simulations of nine experiments, associated with JTWC best-track data from 0000 UTC 2 December to 0000 UTC 5 December 2006.

However, the WSM6-GD combination (Experiment VI) simulated the intensity of 6 hour forecast from 1800 UTC 4 December to 0000 UTC 5 December 2006 in the SCOV. It provided better result than that of other combinations for convective parameterization and analysis. In the accompanying analysis of TC simulation testing, the combination of WSM5-KF, WSM6-KF, WSM6-BMJ and THOM-KF could not simulate the intensity of MSLP, while the WSM5-BMJ and THOM-BMJ combinations simulated better TC intensity than that of previous combination schemes. The V_{max} at 10 meters simulated by the model experiments with above mentioned schemes at 0000

UTC 2 December 2006 and the corresponding observed track data are presented in the middle panel of Figures 5 and 6 (i.e. different spin-up period considerations). The V_{max} during the simulation period obtained from the JTWC best track data was around 90 knots at 1800 UTC 2 December to 1200 UTC 3 December 2006. The THOM-GD combination scheme (Experiment IX) simulated the maximum wind of 87.7 knots, whereas the WSM5-GD and WSM6-GD combination schemes (Experiments III and VI) simulated V_{max} of 76.5 and 78.0 knots, respectively, at 0600 UTC 3 December 2006 for 1 day spin-up time by using the ECMWF-ERAI IBCs.

The combinations of WSM5-KF, WSM5-BMJ, WSM6-KF, WSM6-BMJ, THOM-KF and THOM-BMJ schemes, the V_{max} was underestimated by the WRF-ATM model simulation, especially comparing with the THOM-GD combination scheme. However, the intensity simulated by these three combinations of GD scheme, WSM5-KF, WSM6-GD, and THOM-GD, was relatively similar to the trend of V_{max} for 6 hour forecast from 1800 UTC 4 December to 0000 UTC 5 December 2006 in the SCOV. For the KF and BMJ Cu-convective schemes, the TC simulations presented the lack of exact location, time and intensity by using both IBCs. The KF is indicated as a complex mass flux scheme with closure assumption depending upon the Convective Available Potential Energy (CAPE) removal for an entraining parcel. The BMJ is classified as a convective adjustment scheme for temperature and moisture profiles. The GD is modified for a one-dimensional mass flux scheme in a single updraft–downdraft couplet. In this study, the KF and BMJ Cu-schemes presented a lack of low level convergence and a decrease of convective activity in development of cyclonic system was also shown. The result indicated that the GD combination schemes and their convection with the entire MP-schemes showed better skill for the TC potential track and its intensity at the strong influence of the upwelling area with high SST variability in the SCOV compared with other schemes and observed track data.

3.2. Simulations with Different Spin-up Period, Initial and Boundary conditions

Based on the model results of physical parameterization schemes and their combinations, the model simulation was applied for the TC Durian case study with different spin-up time and IBCs of both global models (ECMWF-ERAI and NCEP-FNL) in order to evaluate the model accuracy and performance testing in terms of location tracking and intensity. Figures 5–7 demonstrate the TC Durian track simulations with different spin-up period and IBCs. All the TC tracking simulations were demonstrated with 72 hour predictions by using the WRF-ATM model consideration from 0000 UTC 2 December to 0000 UTC 5 December 2006 at every 6-hour time interval. It is interesting to note that all pink boxes along the JTWC best-track data are indicated for the time, location and intensity point of the daily consideration under the difference of spin-up period conditions (Figures 5–7).

For the initial study of spin-up processes for tuning up the TC simulation, the WRF-ATM model 15-km grid has "cold started" using both IBCs that are nested to the WRF-ATM 4-km grid. Based on the cold start, a typical spin-up period of approximately 4-6 hours is conducted before the WRF-ATM develops stable, coherent wind and pressure systems. Thus, it could be stated that the forecast guidance is most useful for time periods beyond 6-12 hours. Several researches with 0000 UTC convection-allowing WRF-ATM model simulations revealed that the model could provide very effective guidance for afternoon and evening TC activity [26,27]. A similar spin-up period is, however, explicit in the 1200 UTC WRF-ATM. The useful guidance, thus, might not be provided until the afternoon time period (1800 UTC) at the earliest. In this study, the model testing has been designed for several spin-up experiments in a range of 12-36 hours (e.g. 0.5, 1 and 1.5 days), while the model selection showed only the model convergence which produced the best simulation comparing with the JTWC potential track, V_{max} and MSLP. For the model divergence, the weakness simulation results as a spin-up period for 1.5 days by using the ECMWF-ERAI IBCs and 0.5 days by using the NCEP-FNL IBCs have not been presented in this study.

For both IBCs, the WRF-ATM model has been used for a period of 1 day starting at 0000 UTC 1 December 2006. The second experiment focused on the model generalization capability of speeding up for the model running was also presented in this section. The WRF-ATM model using the

ECMWF-ERAI IBCs started at 1200 UTC 1 December 2006, while the simulation using the NCEP-FNL IBCs began at 1200 UTC 30 November 2006. However, the model experiments using the ECMWF-ERAI IBCs performed well are determining the TC center for 0.5 days and 1 day spin-up periods. Overall, the TC tracks simulated by the ECMWF-ERAI IBCs with both spin-up periods showed better results than those of the NCEP-FNL IBCs comparing with the JTWC observed track. In particular, prior to a 48-hour forecast, the TC tracking error of the ECMWF-ERAI IBCs remained lower than 100 km, while that of the NCEP-FNL IBCs tended to substantially increase with respect to time for all experiments as shown in Figure 7 associated with Tables 3 and 4. Overall, a one-day period of spin-up time taken by the NCEP-FNL IBCs drive to perform the TC tracking location showed northward bias and the TC moved quickly towards land at 1200 UTC 3 December 2006 as compared with the JTWC observed track. The GD combinations of all physical parameterizations in Experiments III, VI, and IX were consistent with the observed track in terms of location tracking for the upwelling area in the SCOV as presented in Figures 5–7 and Table 4. The vector displacement error of TC tracking location under the difference of IBCs and spin-up times is concluded in Figure 7 associated with Tables 3 and 4. The best choice of TC tracking simulation was summarized as the WSM5-GD combination in Experiment III. Mean displacement errors at the 24, 48 and 72 hour forecasts (average daily forecast errors) were 39, 15 and 22 km, respectively, with an entire simulation period of 25.3 km.

The model results of the GD Cu-scheme with three MP schemes have also been consistent throughout the WRF-ATM model experiments with the mean displacement error within 50 km over the 3-day simulation period. It is worth noting that the location tracking errors of model results comparing with the JTWC observed track were different in all the model simulations and varied from 15 to 503 km with an average range from 25.3 to 347.3 km. However, the model could bring these average location errors to the minimum of 25.3 km in a 72 hour forecast at strong influence of upwelling area with high SST variability. The model result, therefore, suggests that the best choice of the model performance testing could minimize the location tracking error and also bring it down to 25.3 km average location error by using the ECMWF-ERAI IBC as shown in Table 3.

In all nine simulations for both IBCs with different spin-up periods, except the entire model simulations of the NCEP-FNL IBCs, the model simulated upwelling areas ahead of the actual site in the SCOV. The location tracking error at the high SST variability significantly decreased from 503 to 22 km on Day 3 (average daily rate) through the simulations from 0000 UTC 2 December to 0000 UTC 5 December 2006. For the analysis of different spin-up periods, the model results clearly illustrated good agreement with the JTWC observed track in terms of location for 0.5 and 1.5-day spin-up periods of both IBCs especially at the first of average daily vector displacement error (Day 1). The TC location tracking error depicted small average displacement errors to 21 km by using the WSM5-GD and WSM6-GD combinations for the ECMWF-ERAI IBCs as shown in Experiments III and VI of the top panel in Figure 7 and summarized in Table 3. It also presented the lowest location error of 46 and 29 km at the last average simulation time (Day 3) in the SCOV as shown in Table 3 and the top left panel in Figures 5 and 7. For the TC simulations of the NCEP-FNL IBCs, the model results presented an overestimation of vector displacement error in terms of location tracking. Their simulation time was also longer than the previous simulation for 12-hour simulation testing. However, the present results indicate that the model shows the moderate location tracking improvement for a 1.5-day spin-up period. The TC intensity study and analysis of V_{max} and MSLP under the Wind-Pressure Relationships (WPRs) have been determined in the next section.

3.3 Analysis of the Relationship between Wind Speed and Pressure

For nine physical parameterizations and their combinations under the difference of global IBCs and spin-up period conditions, the model results and analysis of simulated intensity such as the V_{max} and MSLP have been generally compared to depict the relationship between the TC simulations along with JTWC observed track data for a 72-hour time frame of model consideration (Figures 5 and 6). In this section, the intensity analysis under the WPRs is used to understand the

Preprints (www.preprints.org) | NOT PEER-REVIEWED | Posted: 26 April 2018 doi:10.20944/preprints201804.0336.v1

simulated V_{max} and MSLP results. It was accurately presented in the model comparison of each experiment (Experiments I–IX) with five operational agency equations (Opa.I–V) in term of V_{max} and MSLP for the quadratic curved lines as shown in Figures 8 and 9.

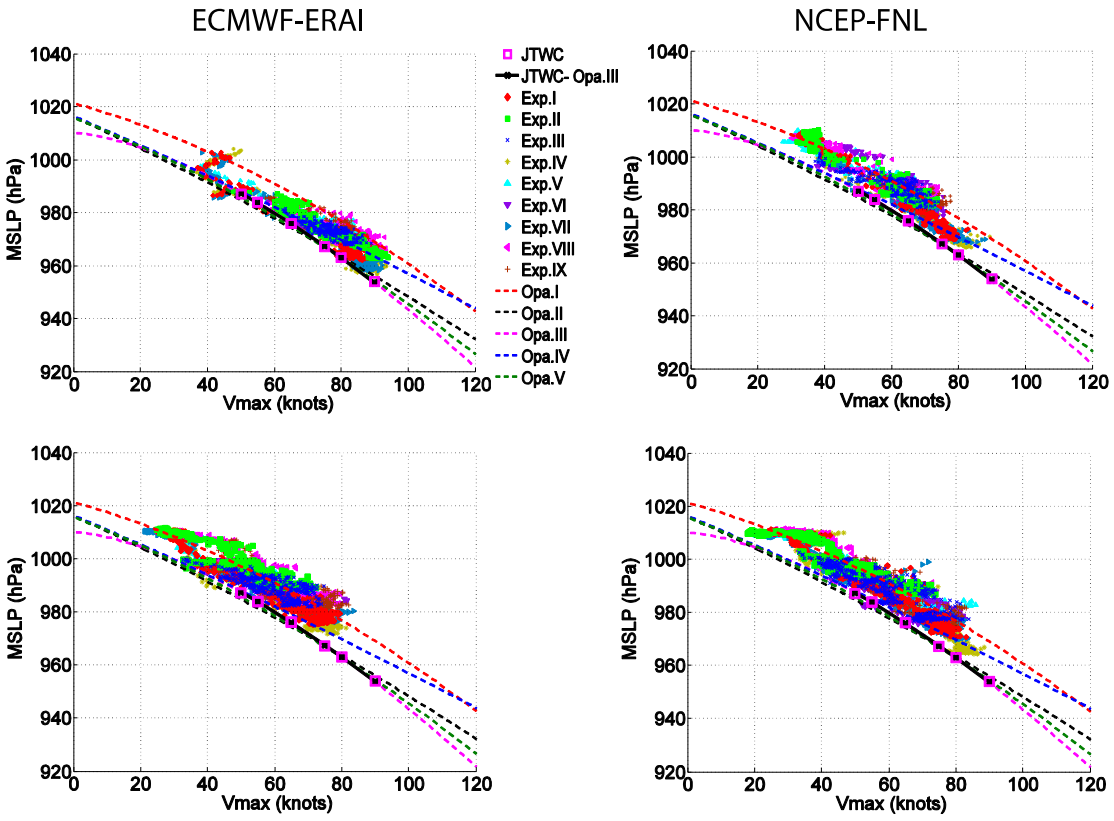

Figure 8. Wind-Pressure Relationships (WPRs) by WRF-ARW model experiments (marker points) by ECMWF-ERAI (left column) and NCEP-FNL IBCs (right column); same (top row) and different (bottom row) spin-up periods, JTWC best-track data (pink squares) with five operational agency curves (dashed line), TC model simulations illustrated by scatter plots for 15 minutes and JTWC curve line recomputed by using the Atkinson and Holliday [23] equation (JTWC-Opa.III as a black cross-solid line).

Preprints (www.preprints.org) | NOT PEER-REVIEWED | Posted: 26 April 2018 doi:10.20944/preprints201804.0336.v1

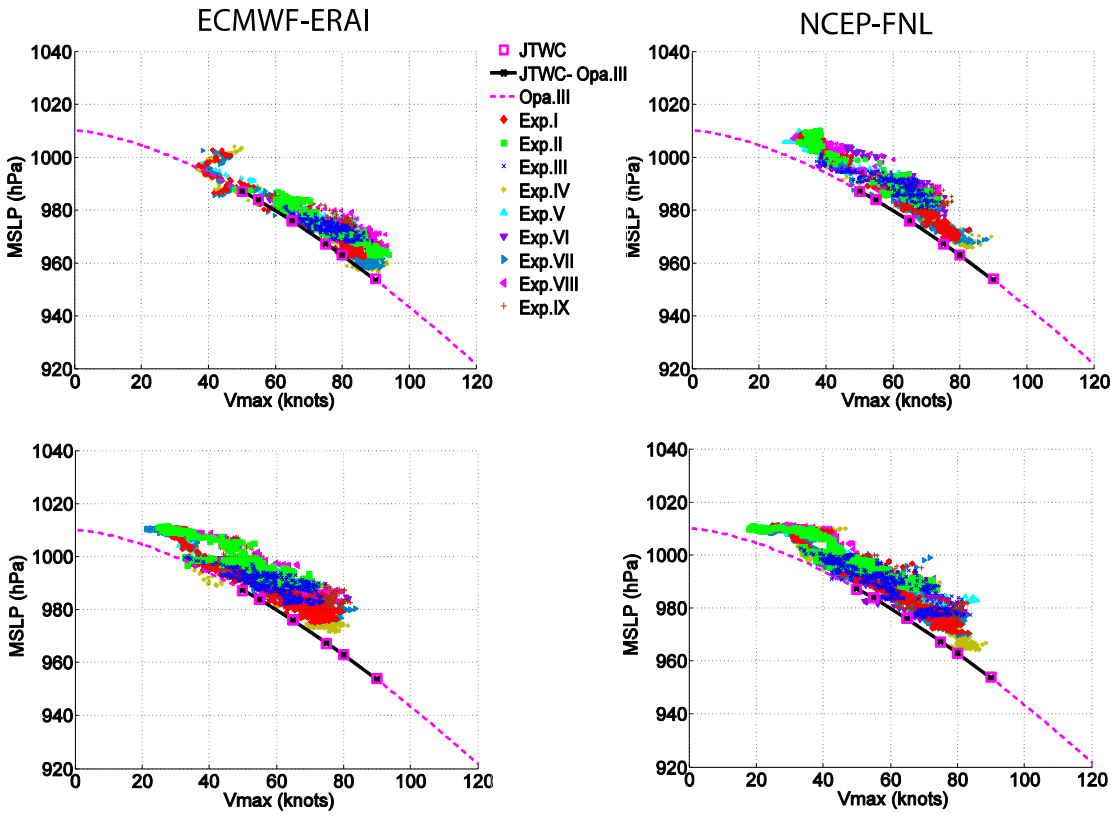

420

421 **Figure 9.** As in Figure 8, but for model results and specify selected by Opa.III and JTWC-Opa.III curve lines for
422 model consideration. The daily intervals of track locations are shown in the pink squares.

423 These figures show that the JTWC best-track data (pink squares) with its black cross-solid line
424 (JTWC-Opa.III) was the general quadratic function which was computed by the Atkinson and
425 Holliday equation (Opa.III). In this study, the intensity simulation of model experiments using the
426 ECMWF-ERAI IBCs with the mapping quantitative data points for 1 day spin-up period was only
427 one of four package sets for the highest consistency of model simulation with five operational
428 agencies (Opa.I–V). In particular, the simulated V_{max} and MSLP showed that the model could
429 capture the TC intensity at peak strength and also under the frame of reference of operational
430 agency curved lines and the JTWC observed data as shown in Figures 8 and 9.

431 The model results of the ECMWF-ERAI IBCs suggest that sampling of TC peak strength could
432 be represented by a full range of intensities which gave sufficient sample size for a 1 day spin-up
433 period. The significant interactivity discrepancies were found in the stronger intensity range. The
434 particular intensified value of the TC simulations tended to present a larger MSLP than that of the
435 observed trend (JTWC-Opa.III). However, the model results of the ECMWF-ERAI IBCs with a 1 day
436 spin-up period represented the best choice of all package sets for decision making under the
437 spin-up period considerations of TC intensity study and analysis. The simulations also show the
438 scatter points closed with the operational agency curved lines which can be directly seen through
439 the data distribution under different spin-up period and IBCs conditions. In addition, the bounded
440 set of scatter simulated results located between five operational agency line curves were the most
441 clearly illustrated guide to the scientific scene of the model simulation and comparison as shown in
442 the top left panel of Figures 8 and 9. The results could be understandably presented by the relation
443 of model scattering points, JTWC intensity points (pink squares) and JTWC-Opa.III observed line
444 by a smooth descending trend of MSLP against V_{max} (black cross-solid line) associated with the

Preprints (www.preprints.org) | NOT PEER-REVIEWED | Posted: 26 April 2018 doi:10.20944/preprints201804.0336.v1

original Opa.III curved line by Atkinson and Holliday equations (dashed line). Furthermore, the larger sequences of gaps between the model experiments and observation were noticed at the scaled main and time frame considerations as shown in the middle and bottom right panels of Figures 5 and 6. The model results also apparently presented an underestimation of V_{max} and overestimation of MSLP under the considerations of model spin-up period, validation and analysis. Explicitly, the simulation results of NCEP-FNL IBCs presented the scatter points spreading out and over the operational agency curved line (Opa.I) by the Dvorak [21] equation as shown in the right panel of Figure 8.

For the ECMWF-ERAI IBCs with 12 hour-spin up period, the results presented low model accuracy as those initialized by the NCEP-FNL IC/BCs. Although the three package sets using different IBCs and spin-up period considerations which simulated the TC intensity showed some deficiencies, they provided some confidence in the ability of model to reproduce located tracking errors for the model study on the spin-up period considerations. Nevertheless, the fact that model results could be presented without the reinforcement of other operational agencies and were understandably illustrated by the simulated V_{max} and MSLP as clearly presented in the top left panel of Figure 9. The results under different IBCs and spin-up period conditions by the WPRs showed that the upper and lower bounds of model simulations were scattered inside the frame of reference for five operational agencies with their curved lines which could predict the cyclone intensity in terms of V_{max} and MSLP (Figure 8).

In summary, the model results have been illustrated in the quadratic curved diagrams by the WPRs (Figure 10). It showed the analysis diagram of MSLP versus V_{max} with the issues of model intensity for the sensitivity results by the smooth ascending and descending trends of both parameters. The curved lines applied by the ECMWF-ERAI IBCs represented the excellent results. It also provided an excellent map with the closed curve of density distribution by comparing with the NCEP-FNL IBCs. In addition, V_{max} and MSLP presented the quantitative dependent variables with the line segment that connected several points on the graph (Figure 9). It expresses a quadratic curve which is interpreted visually relative to both variables under the WPRs as shown in the precise Opa.III equation.

Preprints (www.preprints.org) | NOT PEER-REVIEWED | Posted: 26 April 2018 doi:10.20944/preprints201804.0336.v1

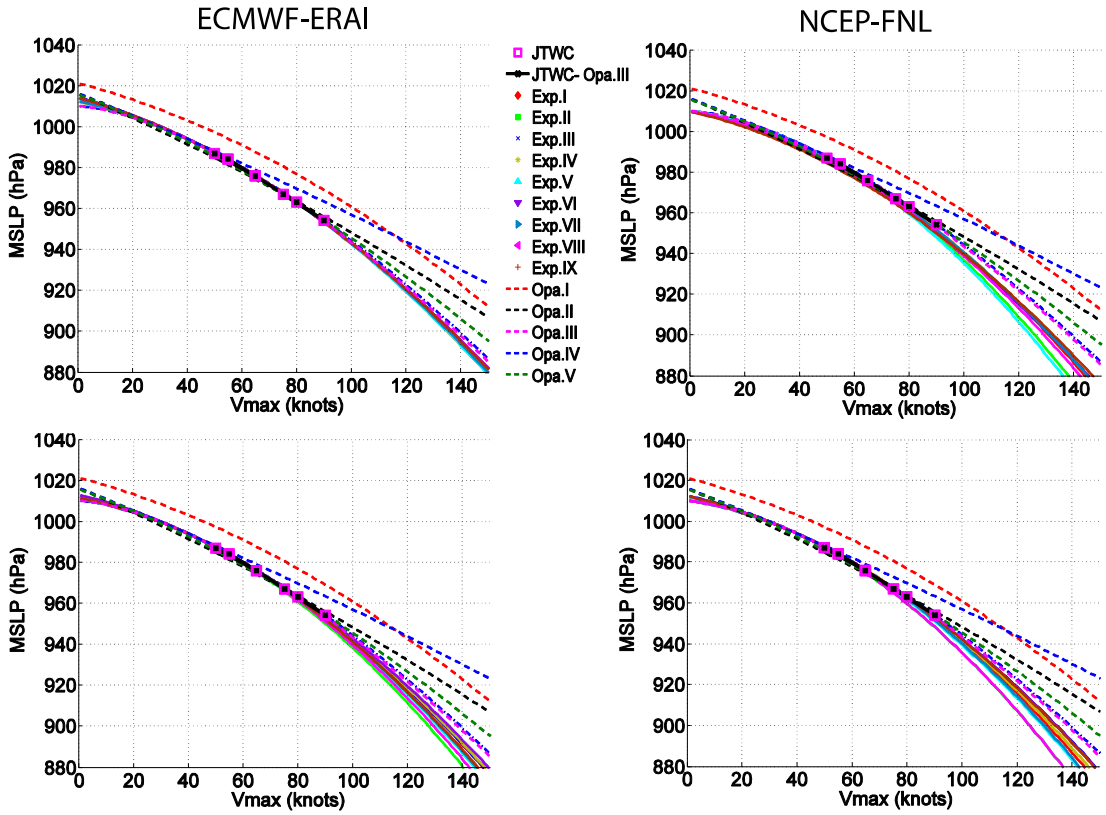

Figure 10. Quadratic curve lines illustrate model experiments (solid lines) by ECMWF-ERAI (left column) and NCEP-FNL IBCs (right column); same (top row) and different (bottom row) spin-up periods, associated with JTWC best-track data (pink squares), JTWC-Opa.III curve line and its smooth descending trend (black cross-solid line) with various five operational agency equations (dashed lines).

Interestingly, the influence of model spin-up period consideration and analysis has a relatively large impact on the reduction of the scatter which described for decreasing the statistical variance explained by the quadratic curved diagram as shown in Figure 10. The model results of the ECMWF-ERAI IBCs with 1 day spin-up period gave the closed curves with the JTWC intensity observed points, JTWC-Opa.III observed curved line and the original Atkinson and Holliday equation (Opa.III). In contrast, the model experiments of the NCEP-FNL IBCs presented the underestimation of simulated results comparing to the JTWC best-track data and the results simulated by the ECMWF-ERAI IBCs. In addition, the model results under the WPRs were finally concluded for the statistical verification and analysis in TC intensity (Tables 5 and 6).

Table 5. Statistical error analysis of V_{max} (in knots) given by MSLP (in hPa) for V_{max} computation with different spin-up periods.

Experiment	ERAI-1 day			ERAI-0.5 days			FNL-1 day			FNL-1.5 days		
	Bias	RMSE	STDE	Bias	RMSE	STDE	Bias	RMSE	STDE	Bias	RMSE	STDE
Exp.I	-1.45	2.64	2.21	-2.16	3.67	2.98	-2.44	4.09	3.27	-3.33	5.53	4.41
Exp.II	-0.72	1.85	1.70	-5.40	8.54	6.62	-5.02	8.15	6.42	-7.40	11.57	8.89
Exp.III	-0.69	1.83	1.70	-2.05	3.55	2.90	-1.91	3.23	2.61	-1.78	3.14	2.59
Exp.IV	-1.49	2.62	2.15	-1.94	3.32	2.69	-2.08	3.51	2.83	-2.68	4.49	3.61
Exp.V	-1.48	2.72	2.28	-3.44	5.58	4.39	-6.10	9.69	7.53	-4.46	7.20	5.65
Exp.VI	-0.75	1.88	1.73	-1.38	2.63	2.24	-1.89	3.25	2.65	-1.84	3.22	2.64

Preprints (www.preprints.org) | NOT PEER-REVIEWED | Posted: 26 April 2018 doi:10.20944/preprints201804.0336.v1

Exp.VII	-1.25	2.34	1.98	-3.15	5.11	4.02	-2.11	3.52	2.82	-4.04	6.64	5.26
Exp.VIII	-0.74	1.85	1.70	-4.26	6.90	5.42	-3.17	5.15	4.06	-7.36	11.56	8.92
Exp.IX	-0.74	1.88	1.73	-2.87	4.76	3.79	-1.22	2.28	1.92	-1.94	3.38	2.77

Table 6. As in Table 5, but for MSLP (in hPa) given by V_{max} (in knots).

Experiment	ERAI-1 day			ERAI-0.5 days			FNL-1 day			FNL-1.5 days		
	Bias	RMSE	STDE	Bias	RMSE	STDE	Bias	RMSE	STDE	Bias	RMSE	STDE
Exp.I	-0.83	1.83	1.63	-1.18	2.28	1.95	-1.17	2.28	1.95	-1.17	2.23	1.90
Exp.II	-0.56	1.67	1.57	-1.48	2.68	2.23	-1.42	2.61	2.18	-1.72	3.01	2.47
Exp.III	-0.43	1.69	1.63	-0.94	2.05	1.82	-1.38	2.58	2.18	-1.04	2.12	1.84
Exp.IV	-0.82	1.85	1.66	-1.06	2.11	1.82	-0.99	2.04	1.78	-1.01	1.99	1.72
Exp.V	-0.96	2.01	1.77	-1.57	2.85	2.38	-1.90	3.27	2.66	-1.16	2.23	1.91
Exp.VI	-0.39	1.66	1.61	-0.64	1.80	1.68	-1.09	2.24	1.95	-0.94	1.99	1.76
Exp.VII	-0.82	1.82	1.62	-1.21	2.31	1.97	-0.95	1.95	1.70	-1.17	2.25	1.91
Exp.VIII	-0.36	1.64	1.60	-1.32	2.46	2.07	-1.59	2.81	2.32	-1.76	3.06	2.51
Exp.IX	-0.35	1.64	1.60	-0.91	2.01	1.79	-0.66	1.83	1.71	-0.87	1.92	1.71

The comparison of intensity simulation of curved line results and observed track reanalyzed by the Opa.III equation was rather small for the model validation. The simulated MSLP tended to be significantly lower than observed intensity with similar V_{max} for the analysis of Bias. The simulation agreed well with the method and analysis results reported by Islam et al. [6]. It was found weakening/steady and intensifying storms had different WPRs and the intensity trend of a given storm was suggested by the shapes of those curves. This was also a key factor to determine the WPRs. Using different IBCs and spin-up periods, the differences found by Atkinson and Holliday [23] were confirmed for the simulation and analysis in this work. The research findings of this study showed that the intensity of storm simulations for a 1 day spin-up period of the ECMWF-ERAI IBCs had a tendency to capture lower pressures and stronger winds comparing with those of other spin-up periods, especially for the model experiments using the NCEP-FNL IBCs with its spin-up periods. The simulated results had a weakening/steady and intensifying for storm considerations. These simulations were further examined in the next discussion of intensity summary and analysis by using the WPRs.

For the WPRs in terms of the statistical analysis indexes (e.g. Bias, RMSE and STDE), the model simulations and observational curved lines by the Opa.III smooth descending trend of V_{max} and MSLP under the WPRs were used to mathematically express a trend of modeling and observational data as summarized in Tables 5 and 6 and corresponded in Figure 10. In this study, the WRF-ATM model experiments indicate that the simulated intensity with different IBCs and spin-up periods by the Opa.III smooth descending trend of V_{max} and MSLP under the WPRs could also be directly influenced by the physical parameterizations and selection through the model experiments. The simulated results with statistical analysis using the WSM5 and WSM6 MP-schemes were found to have lower V_{max} and MSLP than those with the THOM scheme during 3-day simulated time (72 hour forecast) of the super typhoon Durian case study. The results demonstrated that the WSM5

 doi:10.20944/preprints201804.0336.v1

and WSM6 MP-schemes with GD Cu-scheme provided lower accuracy and performance testing than those of the THOM MP-scheme with GD Cu-scheme throughout the entire simulations.

In this study, the summary results show the WPRs curved fitting with V_{max} given by MSLP in nine physical combinations for different IBCs and spin-up period experiments. The WPRs have been used to derive the V_{max} approximations by the statistical analysis indexes as demonstrated in Table 5. The best choice of physical parameterization by the WSM5 and GD Cu-schemes which simulated by using the NCEP-FNL IBCs with 1.5 day spin-up period (Exp.III) provided relatively low Bias of -1.78 knots (RMSE = 3.14, STDE = 2.59). As expected, the model experiment simulated by using the ECMWF-ERAI IBCs with a 1 day spin-up period (Exp.III) yielded the lowest statistical errors in comparison with a Bias of -0.69 knots (RMSE = 1.83, STDE = 1.70). In contrary to derive the MSLP given by V_{max} for the TC reanalysis, Table 6 presents the statistical error of MSLP. The Experiment IX combination with a 1 day spin-up period led the lowest Bias of -0.66 knots (RMSE = 1.83, STDE = 1.71) by the NCEP-FNL IBCs and Bias of -0.35 knots (RMSE = 1.64, STDE = 1.60) by the ECMWF-ERAI IBCs, among all investigated combinations.

In addition, the cyclone made landfall on 5 May 0000 UTC, produced widespread strong winds and pressure drops over the SCOV region. This study discusses the 24-hour location tracking and its intensity such as V_{max} and MSLP from JTWC observed data and model simulated location and intensity for three corresponding days valid at 0000 UTC of 3, 4 and 5 December 2006. In the final analysis, Figures 11–14 represent the 72 hour wind and sea level pressure fields valid at 0000 UTC 5 December 2006 derived from simulated location tracking (pink line), JTWC observed track data (black line) and the final 72 hour simulation of model consideration (pink square) corresponding to the above period of three experiments (Experiments III, VI and IX) from the best choice of model physical parameterizations of full integration system from 0000 UTC 2 to 0000 UTC 5 December 2006.

Preprints (www.preprints.org) | NOT PEER-REVIEWED | Posted: 26 April 2018 doi:10.20944/preprints201804.0336.v1

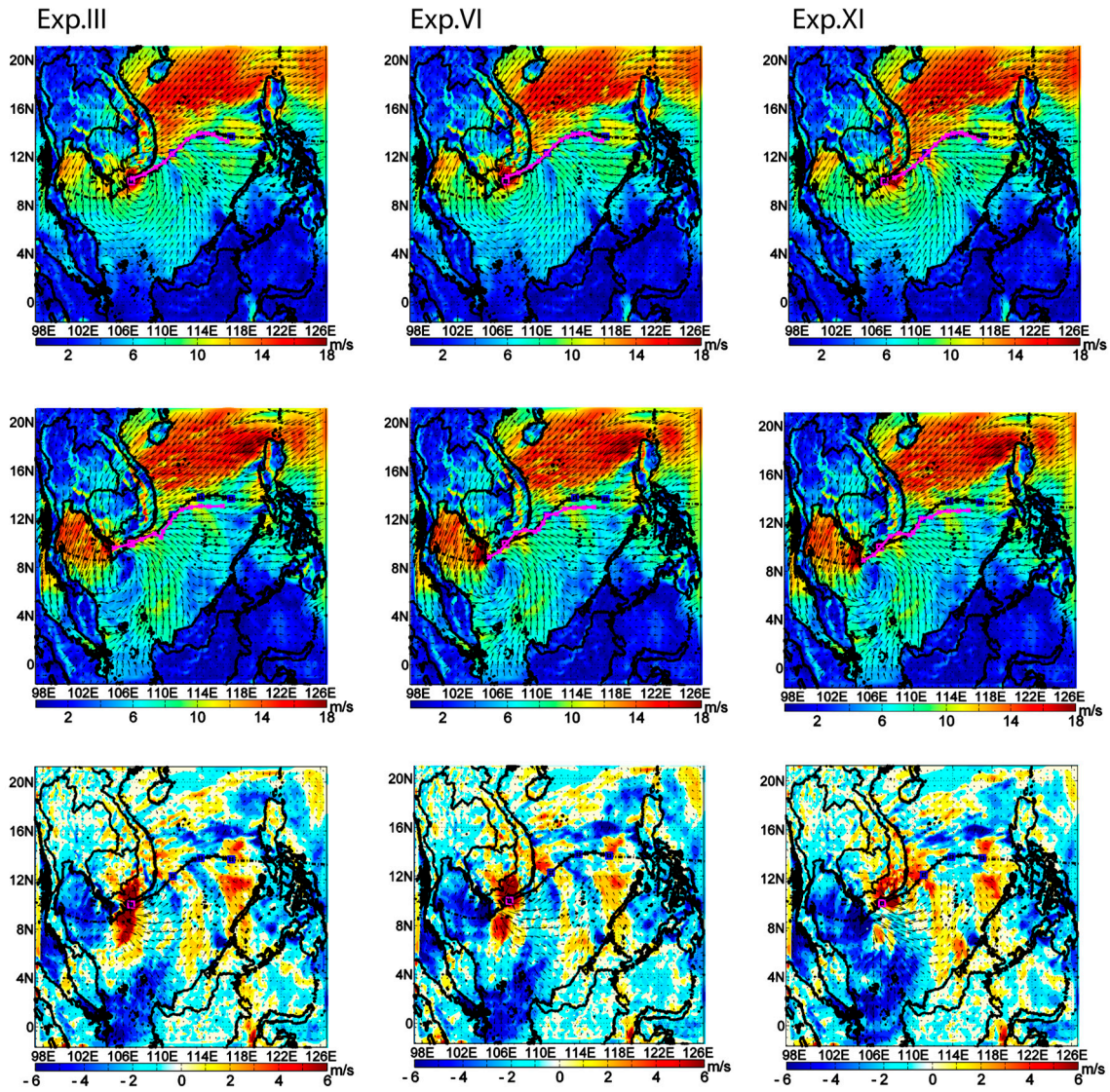

Figure 11. Summary of model experiments in term of wind fields (m/s) at the 10-meter height level selected by model accuracy and performance testing, associated with JTWC best track data (black-solid line). Experiments III, VI and IX with their simulated TC tracks (pink cross-solid lines) by using ECMWF-ERAI (top), NCEP-FNL (middle), and different IBCs (bottom) at 0000UTC 5 December 2006 for 1 day spin-up period.

Preprints (www.preprints.org) | NOT PEER-REVIEWED | Posted: 26 April 2018 doi:10.20944/preprints201804.0336.v1

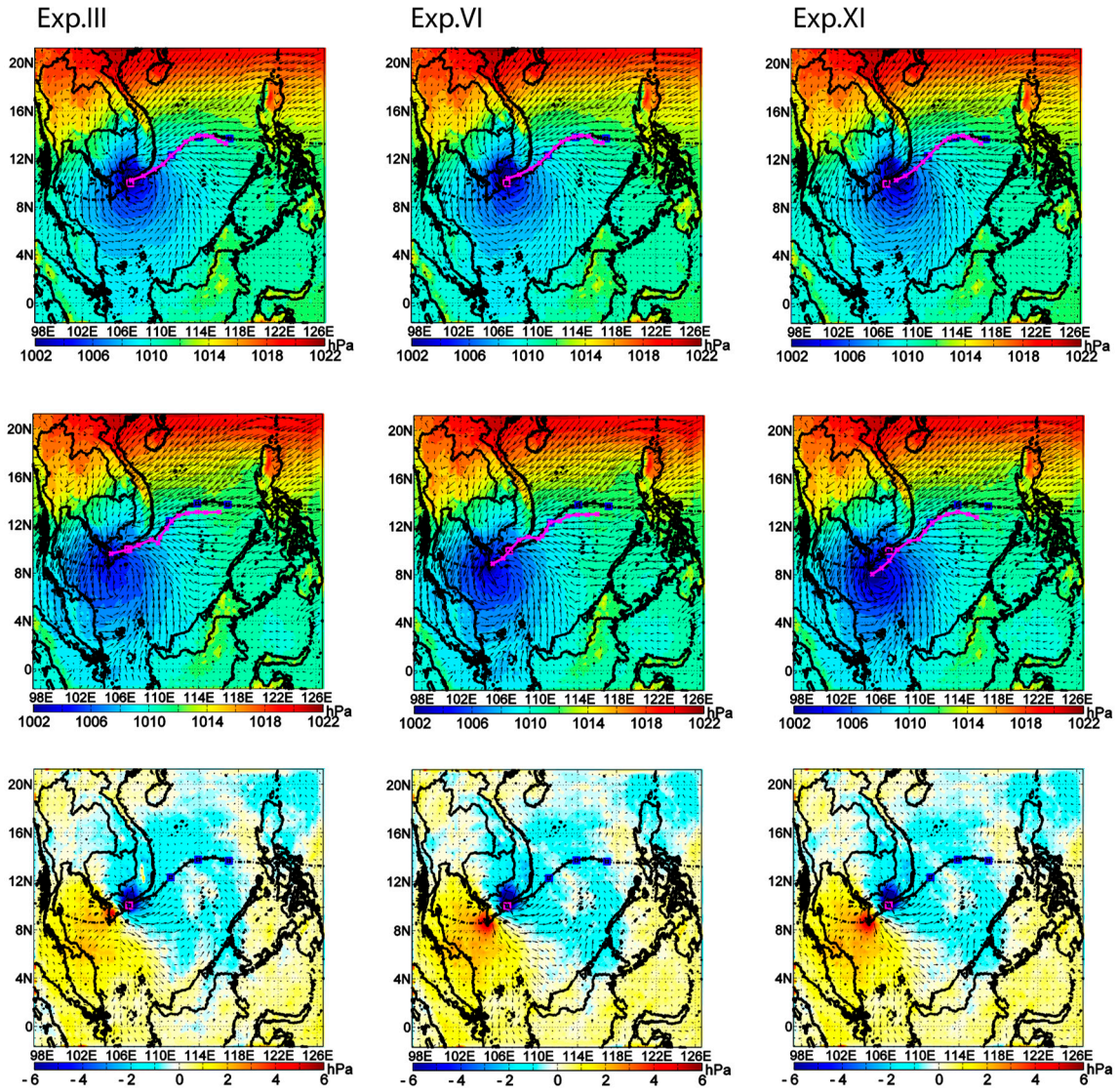

Figure 12. As in Figure 11, but for surface level pressure fields (hPa).

Preprints (www.preprints.org) | NOT PEER-REVIEWED | Posted: 26 April 2018 doi:10.20944/preprints201804.0336.v1

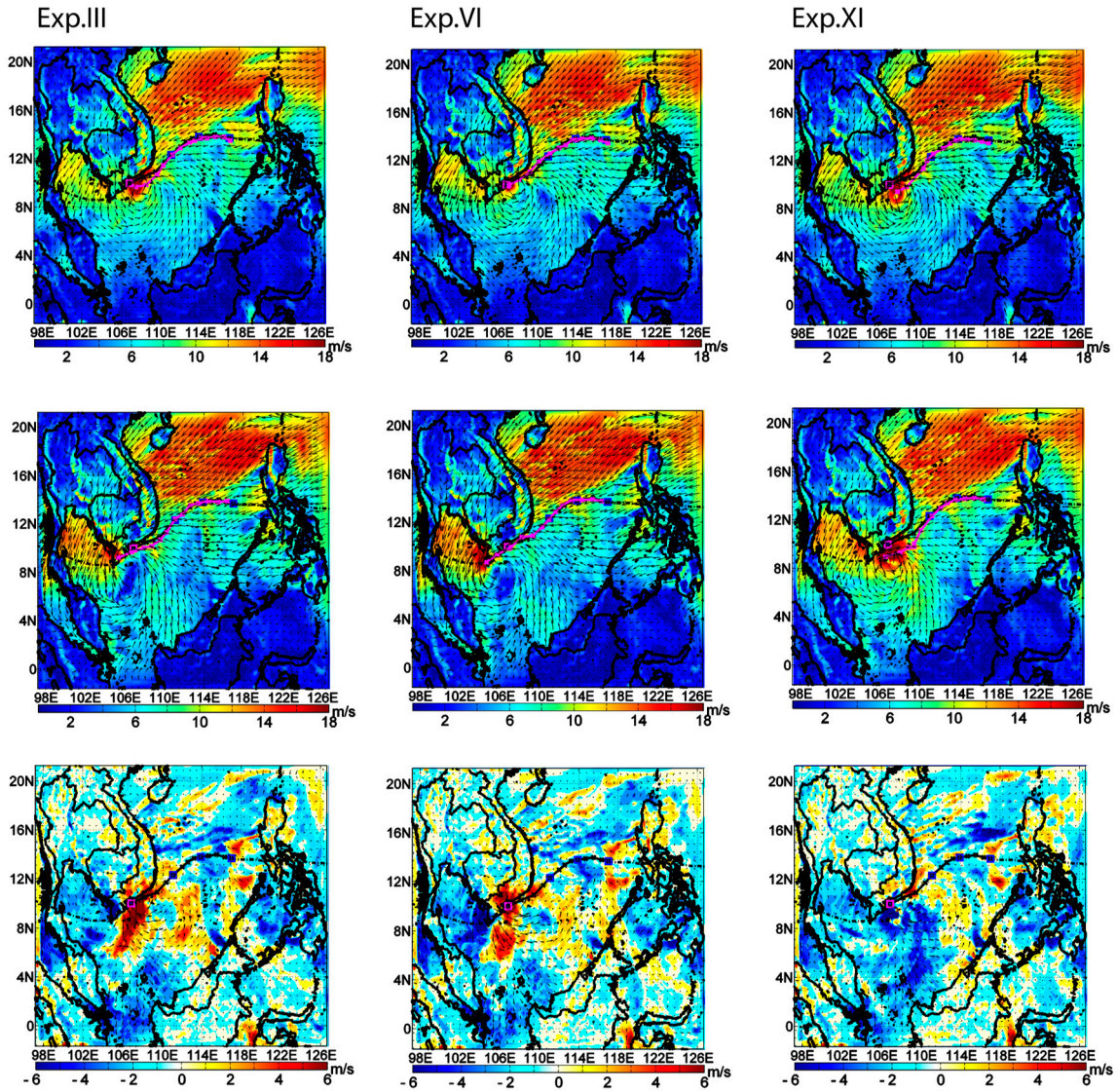

547

548 **Figure 13.** As in Figure 12, but for wind fields (m/s) and its different model spin-up periods of ECMWF-ERAI
549 0.5 days (top), NCEP-FNL 1.5 days (middle) and different IBCs (bottom).

Preprints (www.preprints.org) | NOT PEER-REVIEWED | Posted: 26 April 2018 doi:10.20944/preprints201804.0336.v1

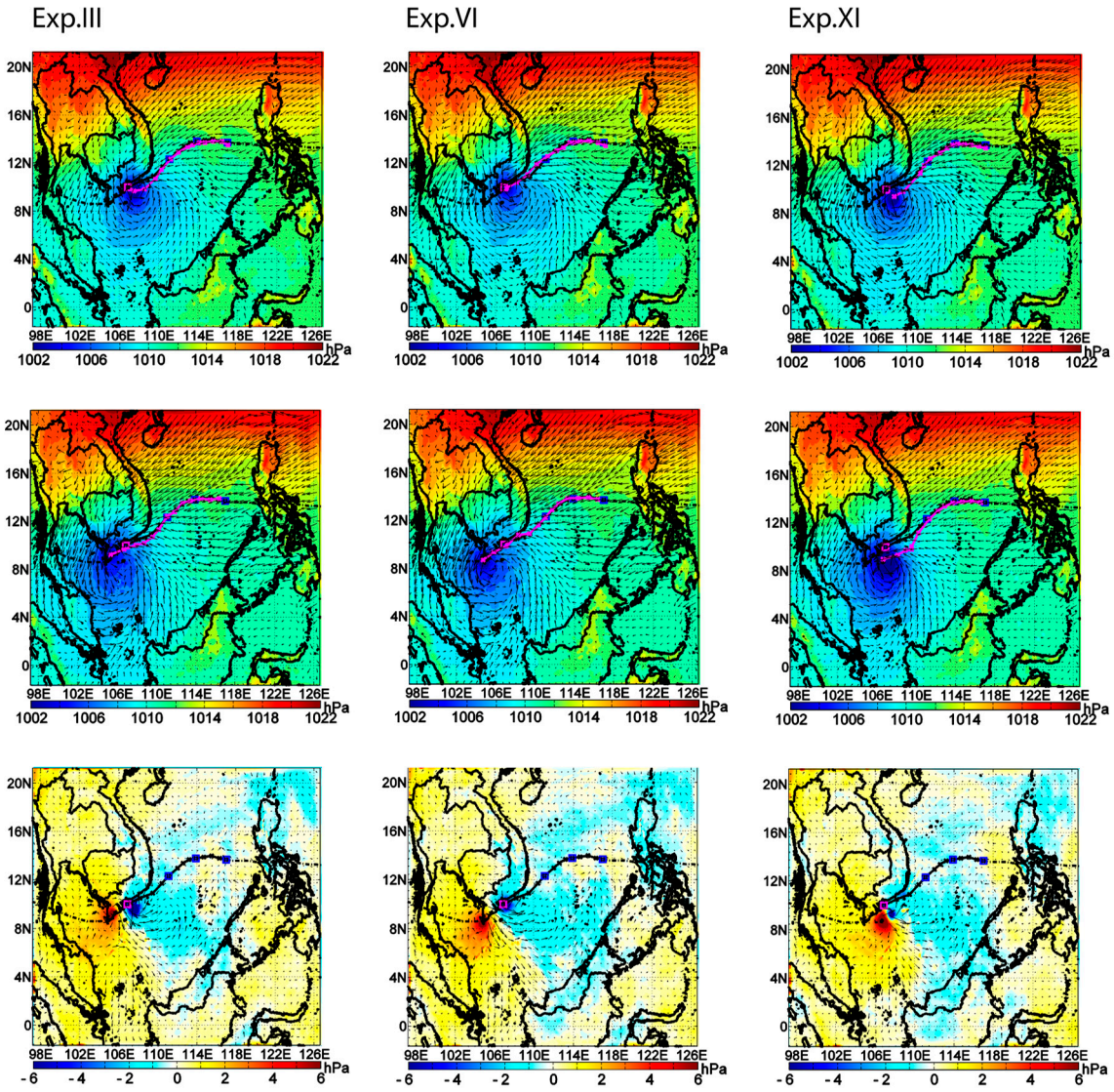

Figure 14. As in Figure 13, but for surface level pressure fields (hPa) and its different model spin-up periods.

In general, the model was able to capture the wind and sea level pressure fields well at the TC center position and can be compared with the JTWC analysis for 3 days. It is noteworthy that the simulations captured the TC center position well at the strong influence of upwelling area with high SST especially in the SCOV by using the ECMWF-ERAI IBCs with both spin-up periods, while it was underestimated by using the NCEP-FNL IBCs. The 24-hour wind and sea level pressure fields at the TC center position valid at 0000 UTC 3 December 2006 from JTWC analysis provided northward bias above the TC simulations by using both IBCs with a 1 day spin-up period in the SCS (Figures 11 and 12). The simulations for Day 1 forecasting from 0000 UTC 2 to 0000 UTC 3 December (average daily rate) capture the TC center position reasonably well by using the ECMWF-ERAI IBCs with 0.5-day spin-up period (Figures 13 and 14). The JTWC intensity for 24-hour analysis valid at 0000 UTC 3 December 2006 illustrated the wind damage associated with increasing TC intensity from 75 (Category 1) to 90 knots (Category 2) over the SCS. In addition, the TC simulation slightly underestimated the V_{max} for the three physical combinations by both IBCs and different spin-up experiments over the SCS. However, the simulations of 0000 UTC 5 December

 doi:10.20944/preprints201804.0336.v1

of a 72-hour forecast shows that the model could capture the TC center position well over the upwelling zone in the SCS, especially for the Experiment III using the ECMWF-ERAI IBCs with a 1 day spin-up period. The wind and sea level pressure fields show high intensity over the SCS, while the TC center position moved toward from the SCS to the GoT. All model experiments, excluding the NCEP-FNL IBCs used (middle panel of Figures 11 and 12) with a 1 day spin-up period of 0000 UTC 5 December of 72-hour forecast agreed reasonably well with the JTWC observed tracking, and successfully predicted the TC location tracking and its intensity of V_{max} and MSLP. However, the Experiment III predicts less MSLP, while the Experiment IX shows the best MSLP results by using the ECMWF-ERAI IBCs with a 1 day spin-up period as the schemes mentioned above. A comparison of the JTWC observed analysis and model prediction indicates that the model was successfully able to simulate the TC location tracking, V_{max} and MSLP in terms of model sensitivity analysis and performance testing as well as intensity. Differences of IBCs, spin-up period and physical combination schemes could provide better understanding of global model uses through WRF-ATM simulation and sensitivity of model physics describing the physical processes in natural phenomena.

4. Conclusions

In this study, the best combination of nine sensitivity experiments on various physical parameterization schemes under the difference of IBCs and spin-up periods for 36 experimental case studies has been performed with the WRF-ATM modeling system to predict super typhoon Durian over the SCS. The model results of the sensitivity experiments revealed that the TC intensity was controlled by cumulus convection and TC track prediction was affected by the microphysics parameterization schemes.

Although the model has underestimated the intensity with all sensitivity experiments, the combination of WSM5 MP-scheme with the GD Cu-scheme by using the ECMWF-ERAI IBCs with a 1 day spin-up period (Experiment III) showed better prediction with MSLP error of 1.69 hPa and V_{max} error of 1.83 knots under the WPRs. The WSM6 and THOM MP-schemes with the GD Cu-scheme for Experiment VI and Experiment IX gave the MSLP error of 1.66 and 1.64 hPa, respectively, whereas the V_{max} error of both experiments was about 1.88 knots - more deviated from the observed data. The dynamical processes of TC location tracking and its intensity were also well captured by the WSM5–GD schemes (Experiment III) in terms of TC center position and V_{max}.

Furthermore, the combination of physical parameterization schemes, the TC simulations were initialized with different IBCs and spin-up period experiments for a 0.5, 1 and 1.5-day model considerations from 0000 UTC 2 to 0000 UTC 5 December 2006. The simulations with various initial conditions indicate that the model is capable of prediction of cyclone intensity in terms of MSLP and V_{max} during the peak period in the SCS and the strong influence of upwelling area with high SST variability in the SCOV. The displacement error of the TC simulation was well predicted by using Experiment III with an average vector displacement error of 25.3 km (approximately 25 km) in 72 hours. The present results demonstrate that the GD scheme and its combinations could successfully predict intensity in terms of MSLP and V_{max}.

Overall, the WRF model shows excellent skill for the TC Durian prediction in terms of location tracking and intensity, suggesting that the model has the potential to be used for operational forecasting systems especially applied for a coupled model with SST updating. In addition, the model could produce the potential and intensities of TC simulation reasonably well over the SCS.

The results of this study would benefit other TC simulations and forecasting under similar conditions to Durian in 2006. In this study, the TC simulation is still a challenging to research and extensive in scope; it is available for model improvement such as precise vortex relocation, model initialization and data assimilation as well as other available observations for fully coupled data assimilation with the TC system developments. The model resolution, various physical

parameterization schemes and IBCs, including realistic steering flow, are important factors of scientific management to successful strategic planning and defense support to cyclone-affected areas. This is especially true in the use of TC warning and prediction systems.

Acknowledgments: The authors would like to acknowledge the Chinese Academy of Sciences (CAS) for a postdoctoral research fund of Worachat Wannawong under the President's International Fellowship Initiative (PIFI) (Grant No.7-158144). We are grateful to Dr. John C. Warner (USGS, Woods Hole) for providing access to the COAWST modeling system. The authors appreciate Dr. Priscilla A. Mooney and Dr. Dave O. Gill (NCAR) for their valuable comments and constructive suggestions on the WRF-ATM model simulations and configurations. Finally, we gratefully acknowledge Michael Willing for his English proof-reading.

Author Contributions: Worachat Wannawong, Yu Zhang, and Chaiwat Ekkawatpanit were responsible for the literature search, setting up the experiments, completing most of the experiments, and writing the manuscript. Donghai Wang principally conceived the idea for the study, the design of the study and provided financial support.

Conflicts of Interest: The authors declare no conflict of interest. The founding sponsors had no role in the design of the study; in the collection, analyses, or interpretation of data; in the writing of the manuscript, and in the decision to publish the results".

References

1. Emanuel, K. *Divine wind: The History and Science of Hurricanes*, 1st ed.; Oxford University Press: NY, USA, 2005; pp. 296.
2. Jansen, M.F.; Ferrari, R.; Mooring, T.A. Seasonal versus permanent thermocline warming by tropical cyclones. *Geophys. Res. Lett*. **2010**, *37*, L03602.
3. Sriver, R.L.; Goes, M.; Mann, M.E.; Keller, K. Climate response to tropical cyclone-induced ocean mixing in an Earth system model of intermediate complexity. *J. Geophys. Res.-Oceans* **2010**, *115*, C10042.
4. Song, P.; Zhu, J.; Zhong, Z.; Qi, L.L.; Wang, X.D. Impact of atmospheric and oceanic conditions on the frequency and genesis location of tropical cyclones over the western North Pacific in 2004 and 2010. *Adv. Atmos. Sci.* **2016**, *33*, 599–613.
5. Warner, J.C.; Armstrong, B.; He, R.; Zambon, J.B. Development of a coupled ocean-atmosphere-wave-sediment transport (COAWST) modeling system. *Ocean Modelling* **2010**, *35*, 230–244.
6. Islam, T.; Srivastava, P.K.; Rico-Ramirez, M.A.; Dai, Q.; Gupta, M.; Singh, S.K. Tracking a tropical cyclone through WRF-ARW simulation and sensitivity of model physics. *Nat Hazards*. **2015**, *76*, 1473–1495.
7. Srivastava, P.K.; Han, D.W.; Ramirez, M.A.R.; Islam, T. Sensitivity and uncertainty analysis of mesoscale model downscaled hydro-meteorological variables for discharge prediction. *Hydrol. Process.*, **2014**, *28*, 4419–4432.
8. Mooney, P.A.; Mulligan, F.J.; Fealy, R. Evaluation of the sensitivity of the weather research and forecasting model to parameterization schemes for regional climates of europe over the period 1990–95. *J. Clim.* **2013**, *26*, 1002–1017.
9. Wang, Y.; An explicit simulation of tropical cyclones with a triply nested movable mesh primitive equation model: TCM3. Part I: Model description and control experiment. *Mon. Wea. Rev*. **2001**, *129*, 1370–1394.
10. Skamarock, W.C.; Klemp, J.B.; Dudhia, J.; Gill, D.; Barker, D.O.; Duda, M.G.; Wang, W.; Powers, J.G. A description of the Advanced Research WRF version 3. *NCAR Tech. Note* **2008,** *NCAR/TN-475+STR*, 113.
11. Nasrollahi, N.; AghaKouchak, A.; Li, J.L.; Gao, X.G.; Hsu, K.L.; Sorooshian, S.; Assessing the impacts of different WRF precipitation physics in hurricane simulations. *Weather Forecast*. **2012**, *27*, 1003–1016.
12. Hong, S.Y.; Lim, J.O.J. The WRF single-moment 6-class microphysics scheme (WSM6). *J. Korean Meteorol. Soc*. **2006**, *42*, 129–151.

13. Thompson, G.; Field, P.R.; Rasmussen, R.M.; Hall, W. D. Explicit forecasts of winter precipitation using an improved bulk microphysics scheme. Part II: implementation of a new snow parameterization. *Mon. Wea. Rev*. **2008**, *136*, 5095–5115.
14. Hong, S.Y.; Dudhia, J.; Chen, S.H. A revised approach to ice microphysical processes for the bulk parameterization of clouds and precipitation. *Mon. Wea. Rev*. **2004**, *132*, 103–120.
15. Chen, F.; Dudhia, J. Coupling an advanced land surface-hydrology model with the Penn State-NCAR MM5 modeling system. Part I: model implementation and sensitivity. *Mon. Wea. Rev*. **2001**, *129*, 569–585.
16. Kain, J.S. The Kain–Fritsch convective parameterization: an update. *J. Appl. Meteorol*. **2004**, *43*,170–181.
17. Janjic, Z.I. The step-mountain Eta coordinate model: Further developments of the convection, viscous sublayer, and turbulence closure schemes. *Mon. Wea. Rev*. **1994**, *122*, 927–945.
18. Grell, G.A.; Dèvènyi, D. A generalized approach to parameterizing convection combining ensemble and data assimilation techniques. *Geophys. Res. Lett*. **2002**, *29*, 1693–1696.
19. Mlawer, E.J.; Taubman, S.J.; Brown, P.D.; Iacono, M.J.; Clough, S.A. Radiative transfer for inhomogeneous atmosphere: RRTM, a validated correlated-k model for the long-wave. *J. Geophys. Res.* **1997**, *102*, 16663–16682.
20. Dudhia, J. Numerical study of convection observed during the winter monsoon experiment using a mesoscale two-dimensional model. *J. Atmos. Sci.* **1989**, *46*, 3077–3107.
21. Dvorak, V.F. Tropical cyclone intensity analysis and forecasting from satellite imagery. *Mon. Wea. Rev*. **1975**, *103*, 420–430.
22. Knaff, J.A.; Zehr, R.M. Reexamination of tropical cyclone wind-pressure relationships. *Weather Forecast* **2007**, *22*, 71–88.
23. Atkinson, G.D.; Holliday, C.R. Tropical cyclone minimum sea-level pressure-maximum sustained wind relationship for western north Pacific. *Mon. Wea. Rev*. **1977**, *105*, 421–427.
24. Xie, S.P.; Xie, Q.; Wang, D.X.; Liu, W.T. Summer upwelling in the South China Sea and its role in regional climate variations. *J. Geophys. Res.* **2003**, *108*, C3261.
25. Zheng, Z.W.; Zheng, Q.N.; Kuo, Y.C.; Gopalakrishnan, G.; Lee, C.Y.; Ho, C.R.; Kuo, N.J.; Huang, S.J. Impacts of coastal upwelling off east Vietnam on the regional winds system: An air-sea-land interaction. *Dynam Atmos Oceans*. **2016**, *76*, 105–115.
26. Kain, J.S. The Kain–Fritsch convective parameterization: an update. *J. Appl. Meteorol*. **2004**, *43*,170–181.
27. Whitaker, J.S.; Hamill, T.M.; Wei, X.; Song, Y.C.; Toth, Z. Ensemble data assimilation with the NCEP Global Forecast System. *Mon. Wea. Rev*. **2008**, *136*, 463–482.